Interactions Between Graphene-Based Materials and Biological Surfaces: A Review of Underlying Molecular Mechanisms

(article starts on next page)

REVIEW

ADVANCED
MATERIALS
INTERFACES
www.advmatinterfaces.de

Check for updates

Interactions Between Graphene-Based Materials and Biological Surfaces: A Review of Underlying Molecular Mechanisms

Yanyan Chen, Santosh Pandit, Shadi Rahimi, and Ivan Mijakovic*

Understanding the underlying molecular mechanism of how graphene materials (GMs) interact with biological surfaces is the key to develop safe and effective biomedical applications of GMs. Here, a systematic and comprehensive mechanistic perspective of interactions between pristine GMs and biological membranes is provided. To this end, first the known mechanisms of interaction between GMs and membrane components are summarized and classified, with a focus on phospholipids, cholesterol, and membrane proteins. Both experimental observations and computational simulations are included. Detailed experimental conditions and physiochemical properties of GMs are listed for each cited application. At the end of this review, current challenges and conflicts that limit biomedical applications of GMs are discussed. Based on reported mechanisms, guidelines for future studies to address the remaining challenges are proposed, specifically with respect to modulating the intrinsic properties of GMs for more efficient and safer therapeutic applications.

1. Introduction

Graphene is a single layered, hexagonally packed 2D carbon sheet that consists of sp^2-hybridized carbon atoms. It has attracted much attention since its first isolation in 2004.[1] The highly conjugated structure gives pristine graphene (PG) a large delocalized electron system, high surface area as well as outstanding electrical, mechanical and photothermal properties, which makes it a promising candidate for applications in many disciplines.[2] However, the inherent hydrophobicity of PG hinders its biological

Y. Chen, S. Pandit, S. Rahimi, I. Mijakovic
Department of Biology and Biological Engineering
Chalmers University of Technology
Kemivägen 10, Göteborg 41296, Sweden
E-mail: ivan.mijakovic@chalmers.se
I. Mijakovic
The Novo Nordisk Foundation Center for Biosustainability
Technical University of Denmark
Lyngby 2800, Denmark

The ORCID identification number(s) for the author(s) of this article can be found under https://doi.org/10.1002/admi.202101132.

and biomedical utility.[3] To improve its poor water dispersibility, direct oxidation of PG is the most feasible and useful method, generating various PG derivatives including graphene oxide (GO), reduced GO (rGO), hydrated GO (hGO), and graphene quantum dots (GQDs).[4] By introducing oxidative groups on graphene sheets through oxidation processes, GO and its analogues usually feature good hydrophilicity and are thereby of great interest for potential utilizations in the biomedical field.[5]

Functionalization of PG derivatives with biocompatible and water-soluble molecules such as chitosan,[6] PEG,[7] and hyaluronic acid[8] is another alternative to overcome their hydrophobicity.[9] With the rapid development of modification methods (noncovalent or covalent) and grafting molecules (polymers or small molecules), the graphene family has been expanded dramatically. Meanwhile, functionalization endows graphene with diverse physiochemical properties, which thereby facilitates graphene materials (GMs)-based applications in biomedical fields.[10] Accompanying the expansion of available GMs, tremendous efforts have also been made to explore broader therapeutic and diagnostic applications.[11] The last few decades have witnessed outstanding performance of GMs in pathogen-killing,[12] cancer therapy,[13] biosensing,[14] drug delivery,[15] cellular signaling,[16] etc.

Despite exciting progress in many areas, there is still a long way to go before applying GMs as biomedicine or biomedical devices in clinic.[17] The fundamental obstacle is the biosafety concern of GMs.[18] Although some publications claimed that GMs were beneficial for the adhesion and proliferation of osteoblasts,[19] stem cells,[20] and cancer cells,[21] many other reports demonstrated that GMs exhibited both short-term cytotoxicity and long-term in vivo damage.[22] The controversy related to biosafety of GMs needs to be cleared in order to pave the way for further biomedical applications. Modification of GMs with biocompatible molecules has been considered as an effective strategy for enhancing the biocompatibility and biosafety of GMs. Nevertheless, the toxicity of GMs remains debatable.[23]

The diversity of GMs arising from non-standardized synthesis and uncontrolled functionalization is one of the major reasons that creates controversy related to the biocompatibility of GMs. Inconsistent protocols implemented by different research groups result in diverse graphene derivatives, which consequently leads to disputable biological responses

**ADVANCED
SCIENCE NEWS**

www.advancedsciencenews.com

**ADVANCED
MATERIALS
INTERFACES**

www.advmatinterfaces.de

and toxicity.[2] Taking GO as an example, the method of production, purity, number of layers, size, and oxidation degree are all important parameters that are closely related to its biological performance.[24] Yet, these physiochemical properties of GO vary extensively from one research group to another. Without standardized production, it is difficult to even identify and characterize these materials, not to mention analyzing their interactions with biological systems.[25] Under these circumstances, it is not surprising that contradictory results co-exist in literature.[24] Some researchers have attempted to classify GMs according to their compositions and physiochemical properties.[26] Hopefully, a clear and unified nomenclature for GMs will be developed in the near future.

The complexity of biological surfaces is another factor that exacerbates the contradictions. For instance, plasma membrane (PM), which consists of a phospholipid bilayer structure with membrane proteins, carbohydrates and cholesterol dispersed on it,[27] acts as the outer boundary of a mammalian cell and thereby interacts with GMs directly. By contrast, cell membranes of most bacteria, fungi, and yeast are usually enveloped by different types of cell walls.[28] Even among bacteria, the cell wall of Gram-negative bacteria differs significantly from that of Gram-positive bacteria. Specifically, the former consists of a phospholipid bilayer and a peptidoglycan layer, while the latter only possesses a thicker peptidoglycan layer.[29] A cell-type-dependent activity of GMs has been reported by many researchers, which fuels the debate on biomedical applications of GMs. Biological membranes not only have complex components that are associated with the cell types, but also have dynamic structures and conformations that vary in response to the external environment and intracellular communications.[30] In order to help future toxicology studies of GMs, we need a more global view of such interaction at the cellular level, as well as a molecular-level understanding of GMs-cell-membranes interaction.

To date, the underlying molecular mechanisms of how GMs interact with cell membranes are still poorly understood.[31] Computational simulations and experimental observations have made some progress in this area. A few reviews have summarized and categorized these interaction mechanisms at cellular level.[32] However, current knowledge regarding molecular-level interactions of GMs and biological surfaces is less organized. Herein, for the first time, we systematically review the recent research progress regarding the interactions between GMs and biological membranes from a perspective of molecular mechanisms and dynamics. For this purpose, we start by listing the known molecular mechanisms of interactions between native (non-functionalized) GMs and several membrane components, including phospholipids, cholesterol, and membrane proteins. The roles of some crucial supramolecular interactions, such as the van der Waals forces, hydrophobic interactions, hydrogen-bonding, and electrostatic interactions, are discussed for each mechanism. Some of the important mechanisms are summarized in **Table 1**. We discuss the structure-property-activity relationships of GMs. Potential guidelines for tailoring the structural properties of GMs for better biomedical application are also proposed. Here we put a particular focus on enhancement of GMs bactericidal activity, minimization of GMs cytotoxicity for mammalian cells, and improvement of GMs selectivity for cancer cells. Finally, we provide new insights into the major knowledge gaps and perspectives for future research.

2. Interaction Between GMs and Phospholipids

Phospholipids are amphiphilic molecules with a hydrophilic head group and two long-alkyl chains as hydrophobic tails.[35] Phospholipid bilayer, also known as the cellular membrane, is the most crucial structure of mammalian and bacterial cells that maintains cell integrity and protects cells from exogenous damage.[36] In this section, six proposed interaction mechanisms between GMs and phospholipids will be introduced: i) inserting/cutting mode, ii) lipid extraction mode, iii) pore formation mode, iv) masking mode, v) lipid peroxidation, vi) electron transfer.

2.1. Insertion/Cutting Mode

The insertion/cutting mechanism was initially proposed by Hu et al. based on experimental observations in 2010.[37] Hu and coworkers noticed severe damage on the cell membrane of *Escherichia coli* under transmission electron microscope (TEM), along with loss of cellular integrity and release of cytoplasm upon exposure to GO, rGO nanosheets, or graphene paper. In line with Hu's report, Akhavan and Ghaderi later found that GO nanowalls (GONWs) and reduced graphene nanowalls (RGNWs) exhibited higher antibacterial activities against *E. coli* and *Staphylococcus aureus* than the suspension of GO and rGO nanosheets (**Figure 1**a).[33] Interestingly, Gram-positive bacteria were more sensitive to both GONWs and RGNWs than were Gram-negative bacteria. The authors attributed the antibacterial mechanism to direct cell membrane damage caused by the sharp edges of nanowalls, which could pierce the cell membrane and insert themselves into it, cutting it like blades. The efflux of RNA provided solid proof for this mechanism. Some perpendicularly orientated nanosheets on the substrate were captured under scanning electron microscope (SEM), which explained the formation of sharp edges (Figure 1b).

Following up on the proven antibacterial activity of GMs, Tu and co-worker investigated underlying molecular mechanisms of such cytotoxicity experimentally and theoretically.[34] Initially, the authors observed that similar GO induced membrane damage on *E. coli* within a certain incubation time (Figure 1c). To explain this behavior via molecular dynamics (MD) simulation, they built all-atom lipid models of both outer and inner membrane of *E. coli*, as well as a graphene model mimicking Akhavan and Ghaderi's experimental condition (deposition of graphene on a stainless-steel substrate). As expected, spontaneous insertion of graphene nanosheets to both membranes was observed during simulation (Figure 1d). Moreover, energy profiles of this insertion mode indicated that strong van der Waals attractions and hydrophobic interactions between graphene and membrane phospholipids were the driving forces that trapped the tail of graphene into cell membranes, followed by the spontaneous rapid insertion of graphene into the cell membranes. Moreover, GO nanosheets in the MD simulation exhibited almost the same behavior as graphene nanosheets. The authors also pointed out that the size of GM nanosheets correlated positively with the extent of lipid extraction.

Although the insertion/cutting mechanism was supported by electron microscopy and computational simulations, it remained unclear whether the sharp edges of GMs contributed

Table 1. The physiochemical properties of GMs, cell lines, and proposed interaction mechanisms.

GMs	Size	Concentration of GMs [µg mL⁻¹]	Incubation time [h]	Interaction mechanisms	Cell lines	Ref.
GO rGO	205 nm	85	2	Mechanical damage and ET	E. coli, A549	[37]
GONWs RGNWs	–	–	1	Mechanical damage and ET	E. coli, S. aureus	[33]
GO	50 nm, 205 nm, 500 nm	100	2.5	Insertion and lipid extraction	E. coli	[34]
PG film	–	–	12	Pore formation	P. aeruginosa S. aureus	[48]
GO	200–700 nm	200	6	Pore formation	A549, Raw 264.7	[49]
GO	0.010–0.7353 µm²	40	2	Wrapping	E. coli	[51]
PG film	–	–	24	ET	E. coli, S. aureus	[60]
Gt GtO GO rGO	6.87 ± 3.12 µm 6.28 ± 2.50 µm 0.31 ± 0.20 µm 2.75 ± 1.18 µm	80	2	Mechanical damage and ET	E. coli	[62]
GO film	–	–	3	Mechanical damage and ET	E. coli	[38a]
GO-S GO-L	50–300 nm 10–40 µm	12.5	3	Cholesterol oxidation	Neutrophils	[68]
GO	800 ± 30 nm	0.5–1	2	Cholesterol extraction	Sperm cells	[69]
GO	1–2 µm	40	24	Activation of TLR4 signaling, Oxidative stress, Impairment of cytoskeleton	J774A.1, Raw 264.7	[70]
S-GO L-GO	50–350 nm 50–1300 nm	20	24	Endocytosis by microphages, Activation of the TLRs and NF-κB pathways	J774A.1	[73]
GO	0.5–4 µm	100	24	Activation of AQP1	MCF-7	[71]
GO	100–300 nm	4 10	24	Activation of integrin-FAK-Rho-ROCK pathway.	J774A.1 A549	[72]

to their bactericidal nature. In good agreement with Akhavan and Ghaderi,[33] some follow-up studies demonstrated the importance of the sharp edges of GMs for their antibacterial activity. Direct experimental data proved that GMs oriented perpendicularly to the bacterial surface had higher antibacterial activity than GMs with random or parallel orientation.[38] By contrast, other reports claimed that it was the basal plane, rather than the sharp edges of graphene, that contributed to the strong interaction between graphene and the lipid bilayer.[39]

Another controversy regarding insertion mode concerned the final/stable configuration of GMs in the membranes. Two possible insertion behaviors have been reported: i) GMs aligned parallel along the midplane of the lipid bilayer and formed a sandwiched graphene-membrane structure (Figure 1e-A); ii) GMs cut across the membrane and ended up with a near-perpendicular configuration (Figure 1d). Titov et al. were the first to simulate an equilibrated graphene-membrane super-structure in a sandwiched configuration. They concluded that this superstructure was more stable than that of graphene inserted vertically into the membrane.[40] Further experimental investigations demonstrated that the configuration of GMs was closely related to the lateral size and the oxidation degree.

According to Li et al., the insertion of micrometer-sized graphene flakes into the membrane started when the sharp edges or corners of graphene oriented nearly orthogonally to the membrane. Then, driven by the attractive interaction between graphene and the tail of phospholipids, graphene migrated until it ended up as an almost perpendicular transmembrane object.[41] Smaller graphene flakes, on the other hand, prefer-entially ended up embedding horizontally in the bilayer and forming the sandwiched structure. This notion was confirmed by Chen et al., who provided experimental evidence for the existence of sandwiched graphene-membrane structure in two mammalian cell lines: the murine macrophage cell line J774A and the murine breast cancer cell line 4T1 (Figure 1e-A,B). Molecular simulation was also employed to support their experimental results.[30c,42] Similar size-dependent insertion behavior was further confirmed by Yi and Gao, who attributed the near-perpendicular penetration of graphene microsheet to the membrane splay and tension energies. Interestingly, they did not report the sandwiched structure proposed previously for small graphene sheets. Instead, a parallel attachment mode on the surface of the membrane was observed.[43] Moreover, Wang et al. proposed that the orientation of graphene relative
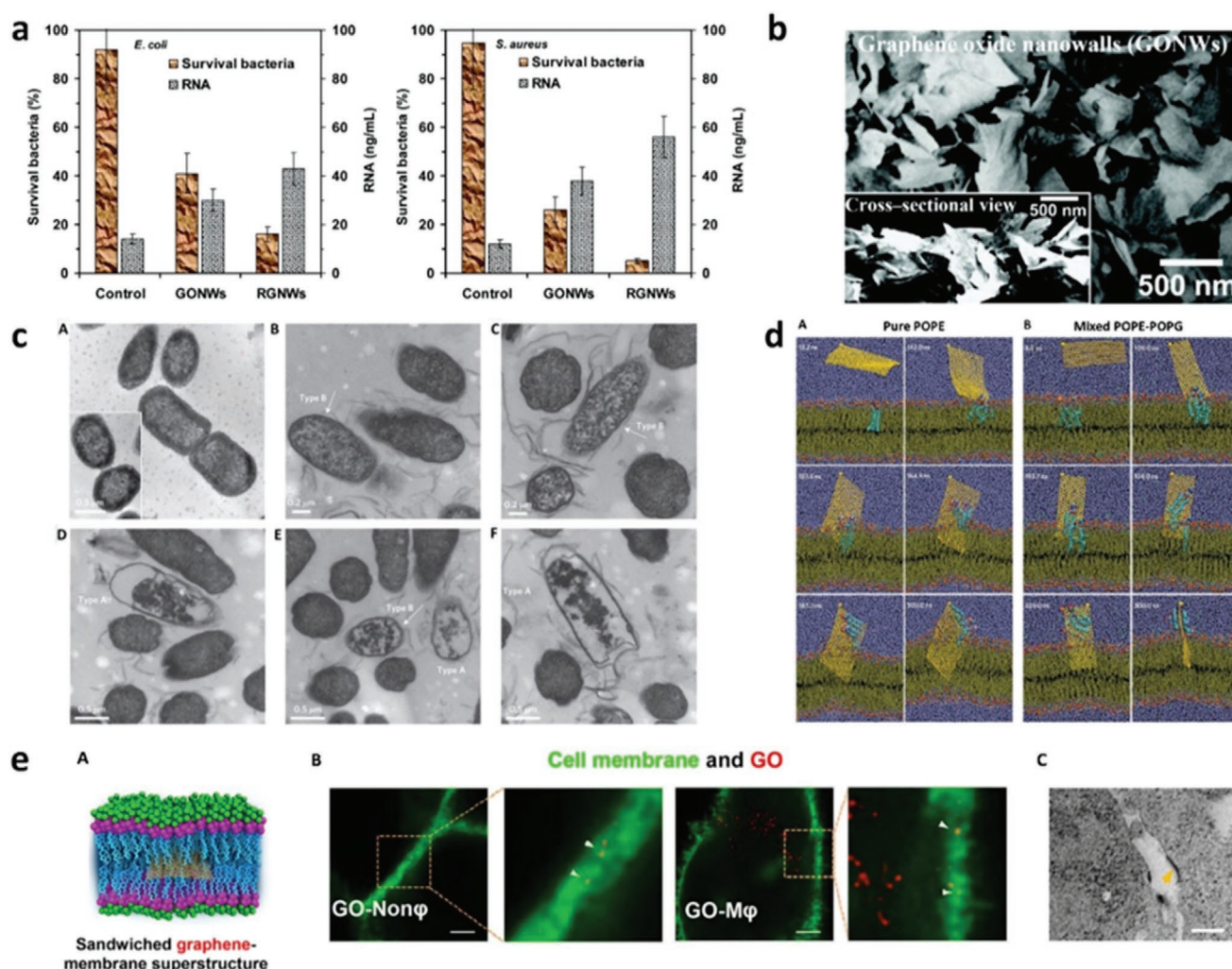
**ADVANCED
SCIENCE NEWS**

www.advancedsciencenews.com

**ADVANCED
MATERIALS
INTERFACES**

www.advmatinterfaces.de

Figure 1. GMs-phospholipids interaction: insertion/cutting mode and lipid extraction mode. a) Cytotoxicity of GONWs and RGNWs to *E. coli* (left) and *S. aureus* (right), along with concentrations of RNA in PBS buffer after exposing bacteria to the nanowalls for 1 h. b) SEM images of the GONWs deposited on stainless steel substrate. Inset: the cross-sectional SEM view of GONWs which indicates nearly perpendicular orientation of GO relative to the substrate. c) TEM images of *E. coli* after incubation with GO (100 μg mL^{-1}) nanosheets at 37 °C for 2.5 h. The morphology changes of *E. coli* can be divided into three stages: A, initial morphology (stage I); B,C, partial damage of cell membranes (stage II), and arrows indicate the "lipid extraction" mode (Type B). D–F, the complete loss of membrane integrity (stage III), where D and F represent the "insertion/cutting" mode (Type A). Both interaction modes are shown in E. d) Representative simulated trajectories graphene nanosheet insertion and lipid extraction in A) the outer membrane and B) inner membrane of *E. coli*. e-A) Cartoon illustration, B) super-resolution confocal images, and C) TEM images of GO-membrane sandwiched superstructure. In confocal images, the green color represents cell membrane, the red spots indicate GO and merged yellow color represents the sandwiched GO in the membrane. Scale bar = 1 μm. a,b) Reproduced with permission.[33] Copyright 2010, American Chemical Society. c,d) Reproduced with permission.[34] Copyright 2013, Springer Nature . e) Reproduced with permission.[30c] Copyright 2019, American Association for the Advancement of Science.

to the membrane was determined by its oxidation degree.[44] Specifically, graphene with higher oxidative level at the edges was showed to pierce into the bilayer membrane and stand across the bilayer, as these edges favored the interaction with hydrophilic head groups of lipids. PG or less oxidized graphene sheets, on the other hand, lay parallel in the middle of the lipid bilayer, which supported the sandwich hypothesis.

2.2. Lipid Extraction Mode

Unlike the insertion/cutting mode which had been confirmed by experiments, lipid extraction was a novel mode. It was

discovered for the first time as a co-existing mechanism with the insertion/cutting mode in Tu's simulation.[34] When contacting a dispersive, flat PG or GO model with inner and outer membranes of *E. coli*, Tu and co-workers found that phospholipid molecules were robustly extracted from cell membranes to both sides of the graphene surface (Figure 1d). Dynamic energy profiles revealed that short-range van der Waals attraction between GMs and phospholipids caused nanosheets to approach and contact the surface of the membranes. Strong adhesion between GMs and phospholipids was able to overcome the hydrophobic packing among phospholipids and played a dominant role for lipid extraction from the cell membrane onto the graphene nanosheet. As lipids kept

**ADVANCED
SCIENCE NEWS**

www.advancedsciencenews.com

**ADVANCED
MATERIALS
INTERFACES**

www.advmatinterfaces.de

moving onto the surface of graphene/GO nanosheets, the nanosheets were dragged toward the membrane, leading to a deeper cell membrane penetration (insertion). Therefore, the authors proposed that this extraction mode co-existed with the previously described insertion/cutting mode. It should be noted that similar lipid-extraction behavior occurred on both outer and inner membrane models, except that the inner membrane featured faster kinetics and stronger lipid extraction compared with the outer membrane. Inspired by these computational results, Tu et al. then verified this lipid extraction phenomena experimentally. The TEM images of *E. coli* treated with GO are shown in Figure 1c. Taking the size effect of GMs into consideration, the authors declared that bigger PG and GO flakes had more phospholipid extraction power (and consequently stronger antibacterial activity) than smaller flakes.

Given that the newly postulated lipid-extraction mechanism was built on a simple graphene model with a flat surface in a dispersed form, limitations to explaining how various GMs interacted with the cell membranes still existed. Thus, extensive studies to expand this model continued. Luan et al. further came up with a wetting-based theory to explain the energetics and dynamics of lipid-extraction process by curved graphene.[45] The authors stipulated that lipid extraction by graphene mainly arose from its hydrophobic surface. During the extraction process, hydrophobic interaction between graphene and the tails of lipids ensured the absorption of lipid onto graphene, while the hydrophilic headgroup of lipid bent toward water. In other words, lipid extraction could be defined as a wetting process (**Figure 2**a). In addition, the curvature of graphene had significant influence on the extraction process. Specifically, lipid extraction preferred occurring on a concave surface of graphene than a flat surface, while barely any phospholipid was extracted on a convex graphene surface. This insight into curvature-dependent lipid extraction might be helpful in designing more efficient graphene-based antibacterial materials.

However, conflicting results on interaction forces involved in lipid extraction mode were reported by Wu et al. using surface-enhanced infrared absorption (SEIRA) spectroscopy.[46] Instead of reliance on the hydrophobic tails of phospholipids, the authors identified that it was the interaction strength between GO and hydrophilic head groups of lipids that drove the extraction process. After probing the molecular interaction between GO and a supported lipid membrane, they concluded that a synergistic mechanism of four weak interactions was the key point for the extraction of phospholipid by GO. These interactions included electrostatic repulsion, electrostatic attraction, hydrogen bonding, and hydrophobic interaction (Figure 2b). Zhang et al. further studied possible influences of oxidation degree of GO on this synergistic mechanism, using SEIRA, confocal laser scanning microscopy and electrochemical impedance spectroscopy.[47] The authors concluded that a delicate balance between the above listed interactions must be maintained in order to obtain a successful extraction of phospholipid. The oxidation degree of GO played a dominant role for the extraction: too few or too many oxygenated groups on the surface of GO might significantly weaken or even eliminate lipid extraction (Figure 2c).

2.3. Pore Formation Mode

Pore formation in cell membranes, caused by graphene nanosheets, was first reported by Pham et al., who performed a series of single-chain main field simulations to study interaction between bacterial membranes and PG.[48] The results surprisingly showed that instead of being simply cut by PG, the lipid bilayer actually could deform to ensure a maximum contact with the lipophilic surface of PG. The deformation thereby induced pore formation within the cell membrane. Furthermore, the authors proposed that these pores could disturb the osmotic pressure of bacterial cells, which might be lethal to the cells. Meanwhile, they observed that after incubating with PG, dead *S. aureus* cells swelled to much larger size than normal living cells, which backed up their pore formation theory (**Figure 3**a).

Later, similar results were reported by Duan and coworkers in different mammalian cell lines.[49] Using electron, optical, and fluorescence microscopy, Duan et al. directly observed plenty of membrane pores appear in GO-treated mammalian cells, such as A549 cells, Raw 264.7 cells, Beas-2b cells, HUVEC cells, and HepG2 cells (Figure 3b). The size and number of these pores kept expanding with increasing dose of GO or with increasing exposure time. However, the mechanism behind membrane pore formation was not clear. Especially, Duan et al. did not observe any pore formation in their previous simulation of graphene-cell membrane interaction.[34] Given that the lipid-extraction mode only involved a single graphene sheet, two parallel-oriented PG nanosheets were then introduced in a new simulation, to mimic the interaction between GO and PM. This simulation demonstrated that cooperative extraction of phospholipids from the cell membrane by multiple graphene nanosheets was responsible for pore formation (Figure 3c). Altogether, the nature of pore formation mode was based on the lipid-extraction mechanism. That is, insertion of multiple graphene or GO nanosheets led to stronger lipid extraction and severe membrane damage, resulting in pore formation.

Interestingly, a MD simulation performed by Chen et al. reported that PG and GO exhibited different behaviors when interacting with lipid bilayer.[50] As shown in Figure 3d, the hydrophobic interaction between lipid tails and PG could drive PG into the bilayer with a parallel orientation relative to lipid tails, regardless of the initial trajectories of PG (vertical or parallel). Additionally, the penetration of PG showed little influence on the integrity of the membrane and no pore formation was triggered by PG. However, due to hydrophilic domains on the surface, GO nanosheets did not insert into the membrane, but rather stayed at the water-membrane interface and extracted phospholipids from the bilayer onto their own surface. This resulted in pore formation and loss of membrane integrity. It is worth noting that the authors did not observe any variation in lipid extraction efficiency related to the size of PG flakes, although they used PG and GO models with three different sizes.

2.4. Masking Mode

The masking effect, referring to an entire cell surface being covered by parallel-oriented GO sheets, was first reported by

**ADVANCED
SCIENCE NEWS**

www.advancedsciencenews.com

**ADVANCED
MATERIALS
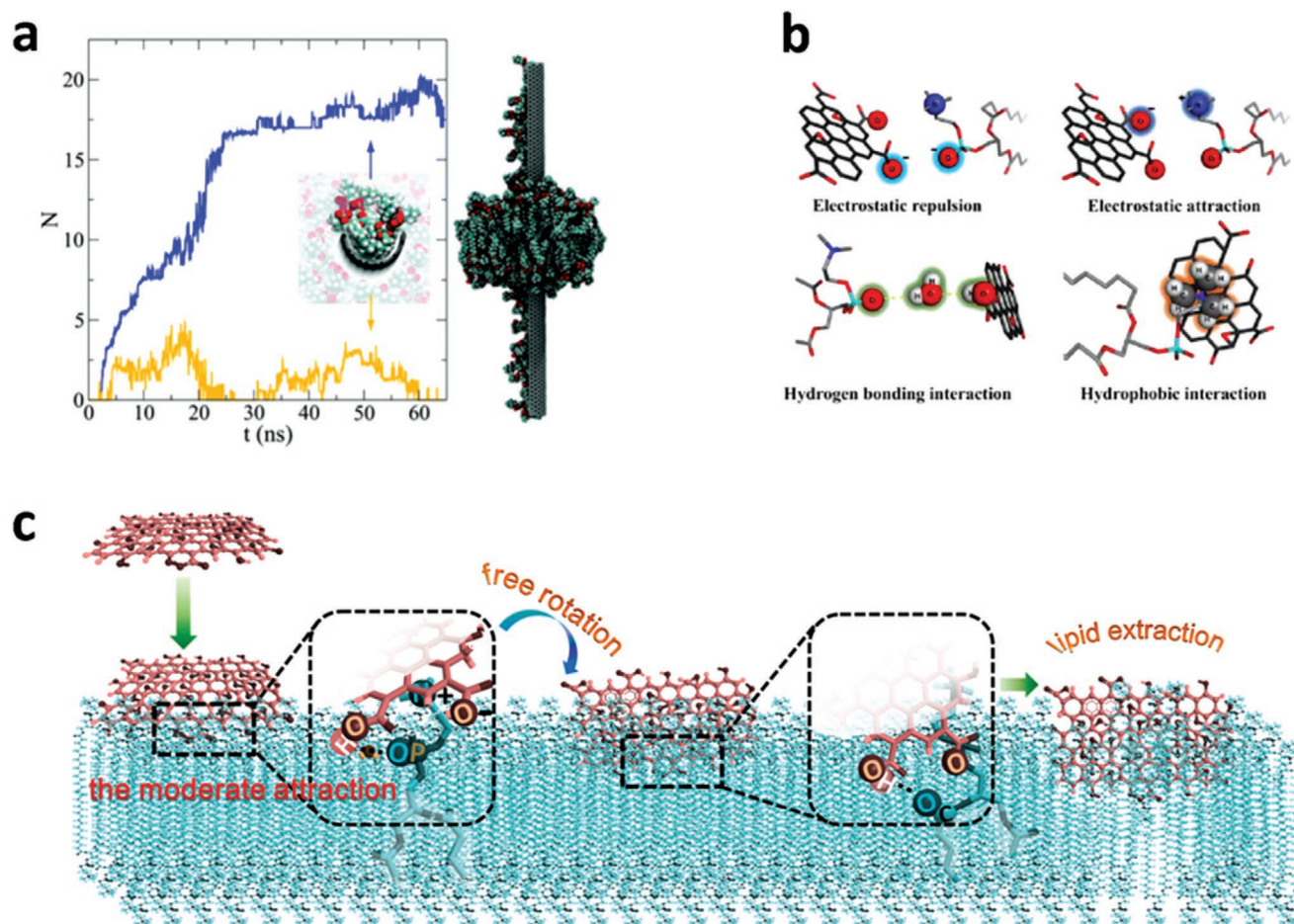INTERFACES**

www.advmatinterfaces.de

Figure 2. GMs-phospholipids interaction: more simulation results of lipid extraction mode. a) The dynamic process of wetting-based lipid extraction by the curved graphene. Left: time-dependent numbers of extracted lipids on the concave surface (blue) and the convex surface (orange) of curved graphene. Inset: a top view of simulation system. Right: a side view of the final state in simulation. b) Schematic diagram of interactions between GO and lipid membrane that contribute to the extraction of phospholipids. c) The synergistic mechanism of weak interactions between GO and lipid membrane that cause the extraction of lipids. a) Reproduced with permission.[45] Copyright 2016, The Royal Society of Chemistry. b) Reproduced with permission.[46] Copyright 2015, American Chemical Society. c) Reproduced with permission.[47] Copyright 2019, American Chemical Society.

Liu et al. in 2012.[51] The authors found that GO flakes exhibited a size-dependent cytotoxicity for *E. coli*. Atomic force microscopy (AFM) was used to investigate possible mechanisms (**Figure 4**a). The results showed that *E. coli* cells were fully wrapped by large GO sheets and isolated from the extracellular environment. The authors argued that this might block membrane transport and even cell proliferation. In contrast, the adherence of small GO sheets on the cell surface could not isolate bacteria. Thus, the bactericidal activity of small GO was weaker than that of large GO sheets. A similar result was reported by Russier in 2013 with the assistance of SEM and Raman spectroscopy. They observed that large GO sheets mask primary human cells and murine phagocytic cells, while smaller GO sheets were mainly internalized by both types of cells.[54]

Besides direct observations, the masking mode was also predicted by several computational simulations. Among these, Dallavalle et al. reported that, in addition to penetrating the membrane, PG could also adhere to the surface of cell membranes and promote translocation of phospholipids (flip-flop)

(Figure 4b).[52] The authors proposed that the overturned phospholipids were responsible for the so-called masking effect of graphene sheets. Moreover, the masking effect was dependent on the size of the PG flakes. Specifically, smaller PG could easily pierce through the phospholipid membrane. As the size increased, strict geometric orientation became necessary for PG to cross the bilayer. However, no piercing behavior was observed for larger PG nanosheets. Instead, they mainly lay flat on the surface of the membrane and flipped the phospholipids underneath (Figure 4c). According to the authors, phospholipid translocation triggered by larger PG reduced the order of cell membrane and eventually wreak havoc to the membrane. However, this contradicted Chen's conclusion that PG exhibited a non-invasive insertion behavior into the lipid bilayer.[50]

Although both experimental and simulated results have been published, demonstrating the masking mode, a reliable molecular mechanism was still lacking. Nevertheless, learning self-assembly behavior of phospholipids on the surface of GMs might help in understanding the masking effect. For this purpose, Hirtz et al. assembled a phospholipid membrane on a
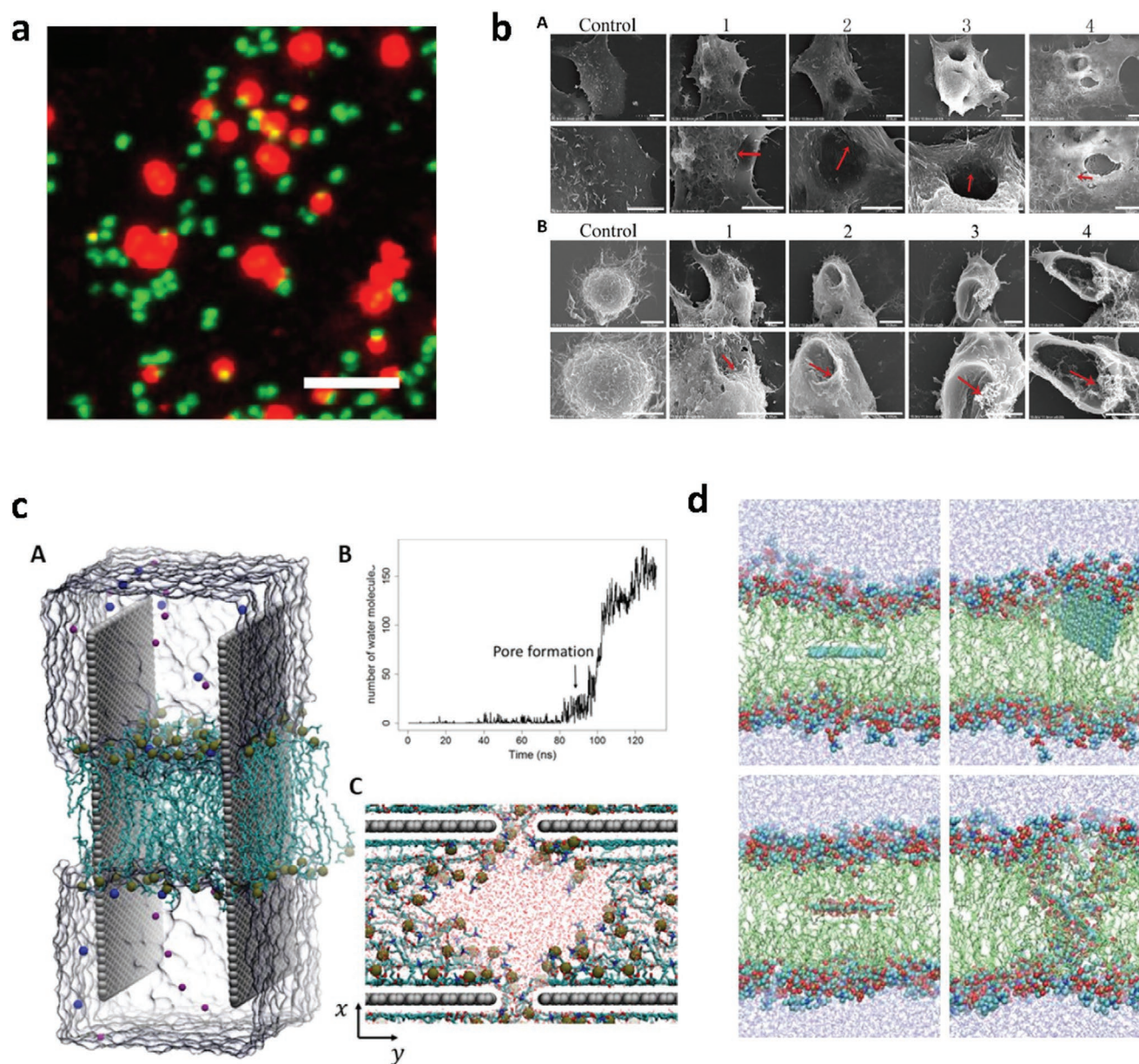
**ADVANCED
SCIENCE NEWS**

www.advancedsciencenews.com

**ADVANCED
MATERIALS
INTERFACES**

www.advmatinterfaces.de

Figure 3. GMs-phospholipids interaction: pore formation mode. a) Live-dead stain of *S. aureus* after the insertion of graphene sheet. Green represents normal, viable cells, while red indicates nonviable cells with increased sizes. Scale bar = 10 µm. b) Morphologies of b-A) A549 and b-B) Raw 264.7 cells under SEM after incubated with GO (200 µg mL^{-1}) for 6 h. Scale bar = 10 µm. The subfigures 1, 2, 3, and 4 represent staged membrane damage during different phases of incubation. c) MD simulation of pore formation process driven by two parallel graphene nanosheets. c-A) Side view of the initial simulation system. c-B) Time-dependent numbers of water influx trough phospholipid membrane after introducing two parallel graphene nanosheets in simulation. c-C) Top view of the final stimulated configuration of membrane pore. d) Different trajectories of interaction between lipid membrane with PG (up) or GO (down), where PG preferred inserting into lipid membrane and located vertically in the membrane, whereas GO could pull lipids out of the membrane onto its surface and thereby induced membrane pore formation. a) Reproduced with permission.[48] Copyright 2015, American Chemical Society. b,c) Reproduced under the terms of the CC-BY 4.0 license.[49] Copyright 2017, The Authors, published by Springer Nature. d) Reproduced with permission.[50] Copyright 2016, American Chemical Society.

graphene substrate to mimic the interface of graphene with cellular membranes using dip-pin nanolithography (DPN).[55] The combination of AFM and Raman spectroscopy was used to examine the layer organization. Using air as the medium, an inverted lipid bilayer structure was captured, with the tail groups of phospholipids oriented toward the graphene support. Upon immersion in different buffers, the preformed inverted

bilayer structure on graphene support reassembled into a phospholipid monolayer structure, exposing the hydrophilic headgroups of lipids to the aqueous solution. According to the authors, the hydrophilicity of the substrate and surrounding environment were crucial for the self-assembly of lipids.

In good agreement with results of Hirtz et al.,[55] Willems and coworkers recently reproduced the self-assembly behavior
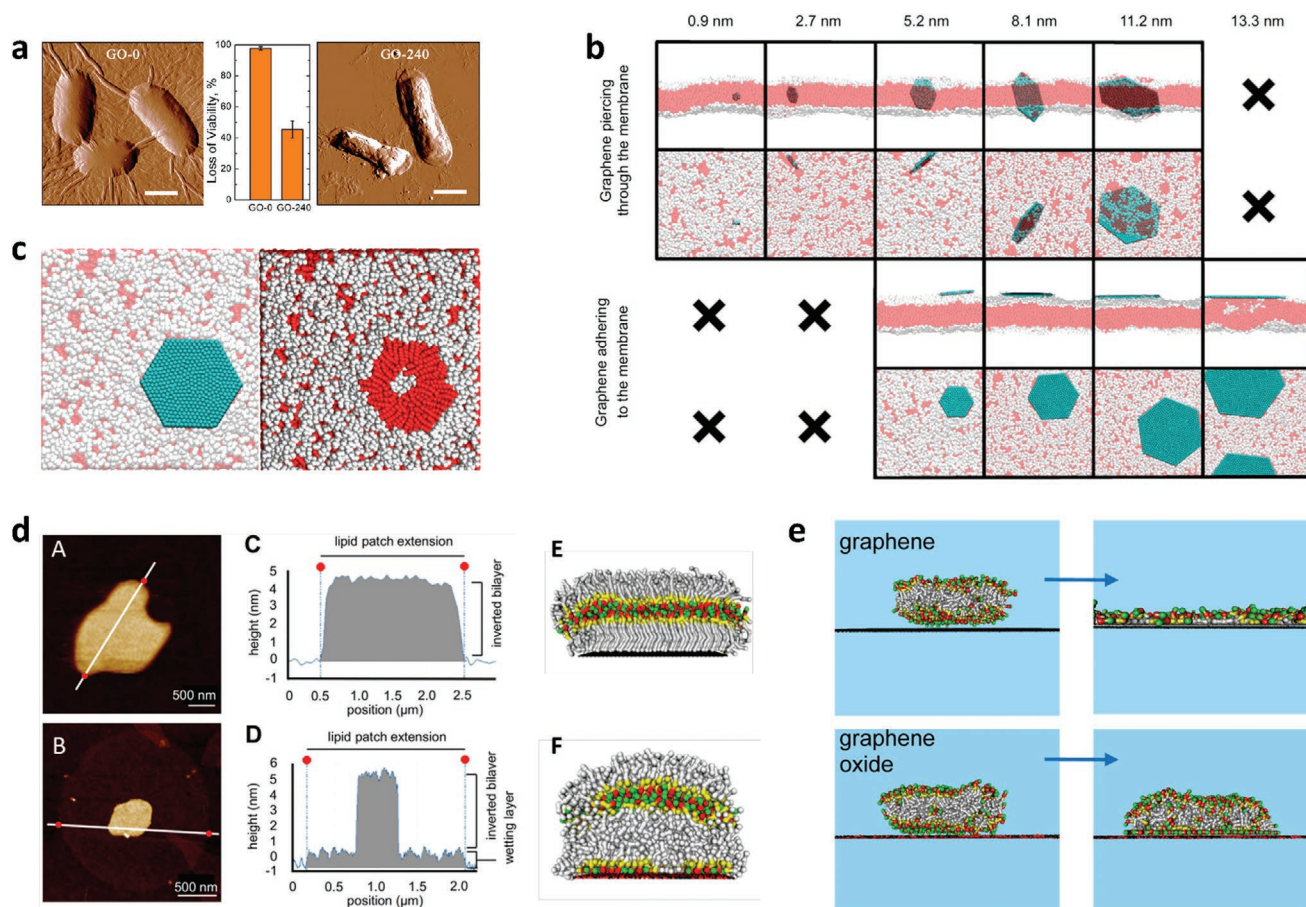
Figure 4. GMs-phospholipids interaction: masking mode. a) AFM amplitude images and cell viability of *E. coli* after incubation with large GO sheets (GO-0) or small GO sheets (GO-240) for 2 h. For AFM image, the concentration of GO suspensions was 40 µg mL^{-1}, while cell viability was determined under 80 µg mL^{-1} GO suspensions. b) Illustrative snapshots of a size-induced piercing through or adhering onto lipid membrane of PG. c) A view of phospholipid membrane when large PG sheet adhered on the surface (left) and a patch of upturned phospholipids on membrane after peeling off the large PG sheet. d) AFM images of L-DPN generated lipid membranes on d-A) PG and d-B) GO surfaces in air with corresponding height measurements (d-C, d-D). d-E,F) Representative snapshot of the inverted lipid bilayer on PG (d-E) and the 1.5 lipid bilayer configuration on the surface of GO in CG-MD simulations. e) Snapshots of the initial and final configuration of CG-MG simulations of lipid bilayer on the surface of PG and GO in water. a) Reproduced with permission.[51] Copyright 2012, American Chemical Society. b,c) Reproduced with permission.[52] Copyright 2015, American Chemical Society. d,e) Reproduced with permission.[53] Copyright 2017, American Chemical Society.

of phospholipids on PG support with a more detailed dynamic process.[53] Additionally, Willem et al. also provided insights into molecular details of lipid interactions with the GO surface, both theoretically (using coarse-grained MD) and experimentally (AFM). In particular, a "1.5 bilayer structure" was obtained on GO surface in air, which consisted of a wetting monolayer with the head groups of phospholipids directly contacting GO surface, and an inverted bilayer on top of this wetting monolayer, as displayed in Figure 4d-F. Interestingly, driven by the interactions between the head groups of lipids and the hydrophilic surface of GO, the preformed 1.5 bilayer structure underwent a spontaneous reorganization with the addition of water into simulation system, forming a stable bicelle-like configuration (Figure 4e). It was noteworthy that the strong hydrophobic interactions between phospholipids and GMs reduced the overall lipid order of the supported lipid membrane, compared to free standing lipid bilayers. Altogether, the reorganization of lipids and reduced lipid ordering caused by PG and GO

might be indicative of what happened to cell membranes in the masking mode.

2.5. Lipid Peroxidation

Besides physical disruption of cell membranes, oxidative stress was another main cause of toxicity of GMs. In the process of reactive oxygen species (ROS)-dependent oxidative stress, ROS generated by GMs resulted in oxidation and damage of components on the cell membrane, as well as intracellular components such as DNA and proteins.[32d] The oxidation of lipids produced several reaction products which were collectively called lipid peroxides. Excessive lipid peroxidation led to membrane disintegration and cell death.[57] Krishnamoorthy et al. reported a very strong bactericidal activity of GO nanosheets based on lipid peroxidation.[58] The observed minimum inhibitory concentration values of GO nanosheets

against *E. coli*, *Salmonella typhimurium*, *Bacillus subtilis*, and *Enterococcus faecalis* were lower than that of kanamycin (a standard antibiotic).[58]

Another report by Li and coworkers explored the relationship between oxidative degree of GMs surface and level of lipid peroxidation in mammalian THP-1 and BEAS-2B cells (**Figure 5**).[56] After comparing the pro-oxidative effects of GO, rGO, and hGO of similar lateral size (100–150 nm), the authors concluded that hGO induced more lipid peroxidation and exhibited higher cytotoxicity than GO. rGO exhibited only minimal effect on cell viability. The increased lipid peroxidation is correlated with the carbon radical density on the surfaces of GMs. The authors then illustrated the whole process of lipid peroxidation: carbon radicals on the basal plane of GMs first donate electrons to surrounding O_2, then ROS is generated and unsaturated lipids that are in contact with GMs are oxidized, yielding lipid peroxides which are responsible for membrane damage and cell death. It has been demonstrated that the density of carbon radical on the surface of GO is closely correlated with their carbon to oxygen ratio (C/O).[59] By manipulating the oxidative groups and oxidative degree of GO, proper radical

content can be achieved easily, which facilitates the biological applications of GO.

2.6. Electron Transfer

Electron transfer (ET) from bacteria to GMs was proposed to kill bacteria by disturbing, oxidizing, or depleting vital cellular structures or components. ET induced oxidation was a ROS-independent process, which might induce degradation of intracellular molecules and thereby kill cells. The fundamental basis of the ET mechanism was that bacteria tended to exchange electrons with the external environment through their respiratory chains located on their membrane. GMs could interfere with the activity of the respiratory chain. To achieve efficient ET, direct contact between bacteria and GMs was required.

Currently, only a few reports on ET between GMs and bacteria are available. Most of these reports did not provide direct evidence for ET causing cell death. Instead, they offered indirect evidence, showing that GMs could oxidize glutathione (GSH) in buffer solution without producing much ROS. In
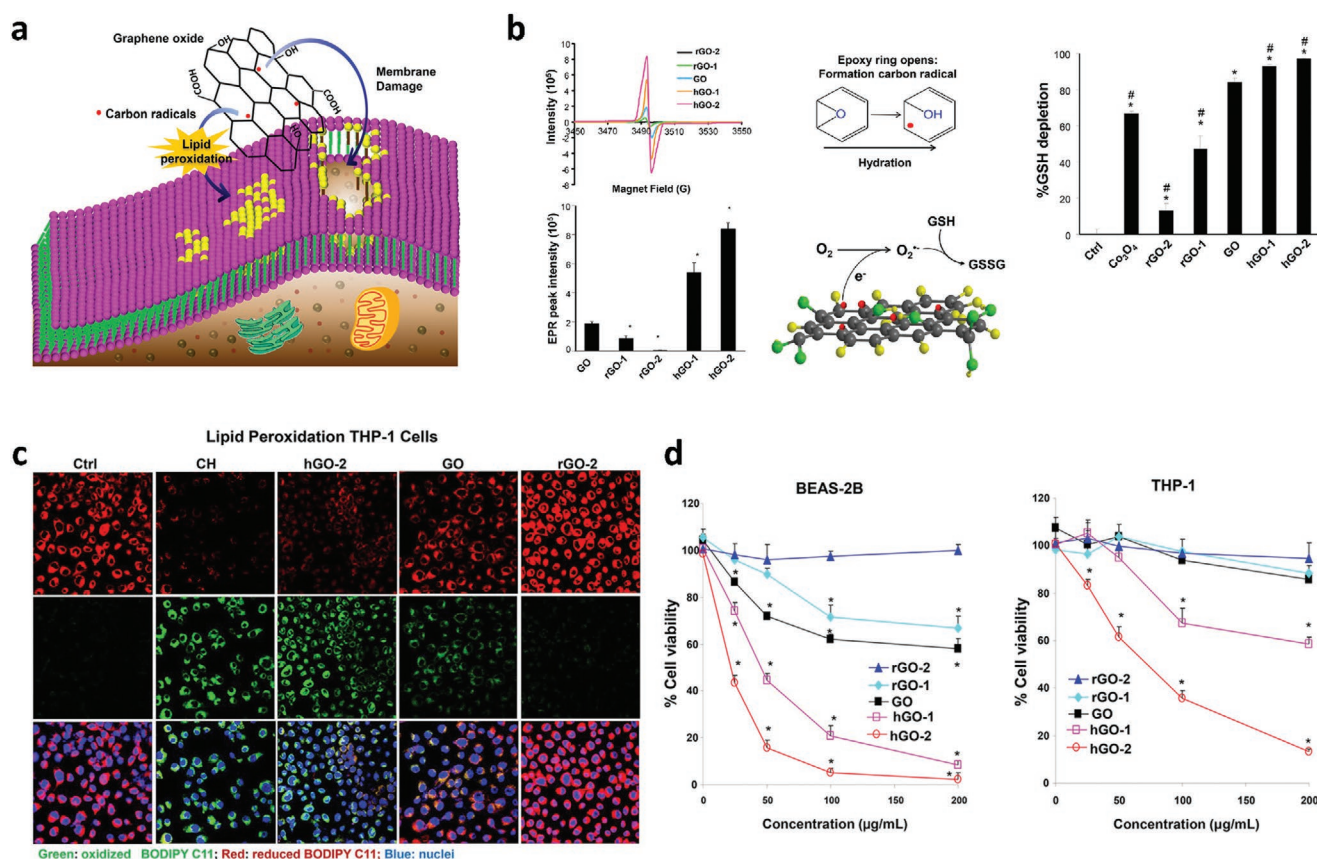

Figure 5. GMs-phospholipids interaction: lipid peroxidation mode. a) Schematic illustration of GO induced lipid peroxidation and cell membrane damage. b) Left: assessment and quantification of carbon radicals on the surfaces of different GMs by electron paramagnetic resonance. Middle: scheme of the generation of carbon radicals during hydration reaction for the synthesis of hGO as well as the subsequent ROS generation and GSH oxidation. Right: GSH depletion assay for GO samples of different oxidation levels. c) Confocal images of THP-1 cells incubated with 100 µg mL^{-1} GO samples for 16 h and then co-stained with a lipid peroxidation sensor BODIPY 581/591 and a nucleic acid stain Hoechst 33342 to evaluate lipid peroxidation. Cumene hydroperoxide was used as a positive control reagent. d) Cell viability assessment for THP-1 and BEAS-2B cells. The cells were cultured with five GO suspensions of varied concentrations (0, 50, 10, 200 µg mL^{-1}) over 48 h. Reproduced with permission.[56] Copyright 2018, American Chemical Society.

ADVANCED
SCIENCE NEWS
www.advancedsciencenews.com

ADVANCED
MATERIALS
INTERFACES
www.advmatinterfaces.de

2011, Liu et al. cited a "three-step antimicrobial mechanism" of carbon nanotube (GMs-cell membrane contacting, membrane stress caused by sharp edges, oxidative stress caused by the ET) to explain the different cytotoxicity of GO, rGO, graphite (Gt), and graphite oxide (GtO). The authors attributed stronger cytotoxicity of conductive Gt than insulating GtO to a better ET between Gt and the membrane of *E. coli*, which was demonstrated by a higher GSH oxidation capability of Gt.[62] But ET seemed not to be the dominant antibacterial mechanism in this study, since GO showed highest bactericidal efficiency although it oxidized less GSH than rGO or Gt. This suggested a synergistic antibacterial effect, in which dispersibility, size, surface roughness, and oxidative level, all contributed. Similar experiments were performed by Lu et al. and conclusions supported the synergistic killing mechanism of vertically aligned GO nanosheets against bacteria.[38a]

To provide more direct evidence for the ET mechanism, Li et al. compared bactericidal effects of flat graphene films on conductor Cu (Graphene@Cu), semiconductor Ge

(Graphene@Ge), and insulator SiO$_2$ (Graphene@SiO$_2$).[60] The results illustrated that Graphene@Cu and Graphene@Ge could induce obvious membrane damage to both Gram-negative and Gram-positive bacteria, while hardly any bacteria were killed on Graphene@SiO$_2$ (**Figure 6**a,b). After studying the energy band of graphene/substrate junctions, the authors therefore attributed the differences in cell viability to ET from bacterial membrane to the graphene film. They explained that with a conductive substrate under the graphene film, an electrical circuit could be easily formed due to ET from the bacterial membrane to graphene. This electrical circuit then led to membrane damage and eventually cell death. Conversely, no electrical circuit was formed for bacteria contacted with insulating Graphene@SiO$_2$, and neglectable bactericidal activity was detected in that case (Figure 6c). Despite the demonstration that ET occurred between bacteria and GMs, the understanding of ET mechanism on molecular level was still far from adequate.

A very recent report by Wang et al. regarding bacterial detecting and killing based on ET from bacteria to an
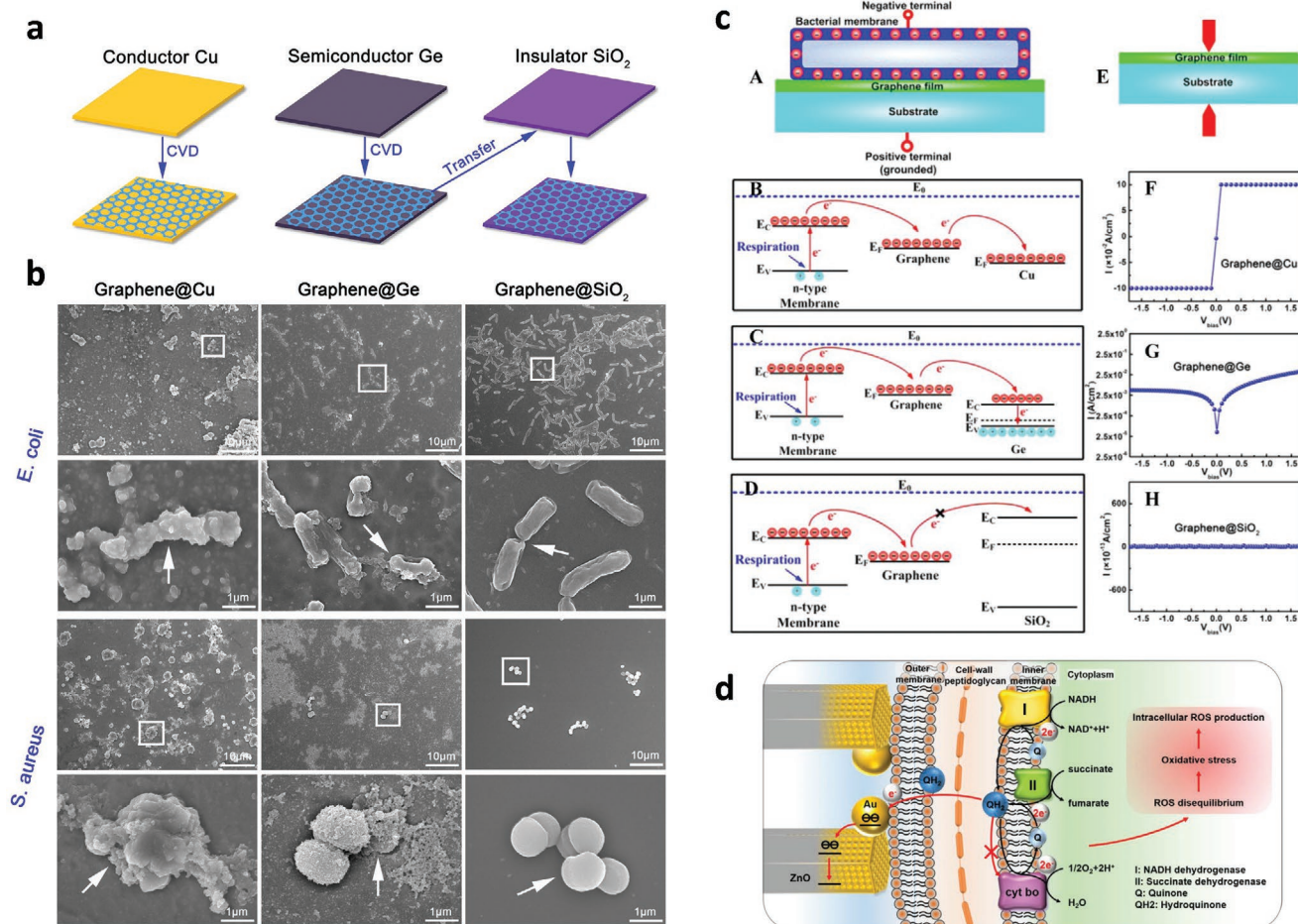

Figure 6. GMs-phospholipids interaction: ET mode. a) Schematic illustration for the fabrication of monolayer graphene films on substrates including conductor Cu, semiconductor Ge, and insulator SiO$_2$. b) SEM images of *E. coli* and *S. aureus* cells that were seeded onto the graphene films coating on different substrates. The rectangular areas were magnified for high resolution images. c) Schematic circuitry to illustrate the ET mechanism from the view of the energy band diagrams of these graphene-on-substrate junctions (A–D); Scheme for the electrical measurements (E) to obtain the current–voltage characteristics of three different contacts of graphene films with the underlying substrates (F–H). d) Schematic illustration of ET from *E. coli* to Au@ZnO that led to death of bacteria. a–c) Reproduced with permission.[60] Copyright 2014, Springer Nature. d) Reproduced with permission.[61] Copyright 2020, Wiley-VCH.

Au-loaded semiconductor (ZnO) provided a more detailed ET route (Figure 6d) : electrons were first generated by dehydrating NADH and succinate, then captured by electron acceptors such as quinone, and finally passed to the surface of semiconductor.[61] The interference with the membrane respiratory chain consequently caused membrane stress, affected subsequent signaling pathways, accumulated ROS inside cells, and finally triggered cell death. This work may inspire future investigations of the EF process between bacterial membranes and GMs.

2.7. Other Mechanisms (Based on Liposome Model)

Since the study of graphene-cell membrane interaction is still at a very early stage, MD analyses so far usually employed a single graphene nanosheet with a certain size (more particularly, very small relative to the size of the whole cell model) and a fixed orientation relative to the lipid bilayer. However, in experiments and applications, size, orientation, aggregation, and lipophilicity of GMs were diverse and complex, which might lead to very different interactions between GMs and cell membranes.

To address this, Li and coworkers recently constructed a more comprehensive simulation system to investigate the interaction between hydrophobic nanosheets and lipid membranes.[63] Specifically, a spherical liposome model was employed to mimic the 3D structure of a cell. The size of nanosheets ranged from smaller than the thickness of the lipid membrane to larger than the entire liposome. The nanosheets were positioned both perpendicular and parallel to the lipid membrane in the initial states of simulation. In total, five liposome-nanosheet interaction states were captured, which were insertion, corrugated insertion, split, corrugated sandwich, and collapse. Behind these states, several molecular mechanisms were involved, including nanosheet rotation, lipid flip-flop, lipid extraction, and lipid spreading. The results are summarized in **Figure 7**.

Among these mechanisms, most of them (e.g., nanosheet rotation, lipid insertion, and extraction) were in agreement with previously reported results. The authors propose that "lipid spreading" was consistent with Hirtz's results,[55] though they did not use the same term. However, the understanding of lipid flip-flop mechanism here was not exactly the same as described by Dallavalle and coworker, who defined the overturning of phospholipids below graphene as flip-flop.[52] By contrast, Li et al. stated that lipids beneath the nanosheet were pressed
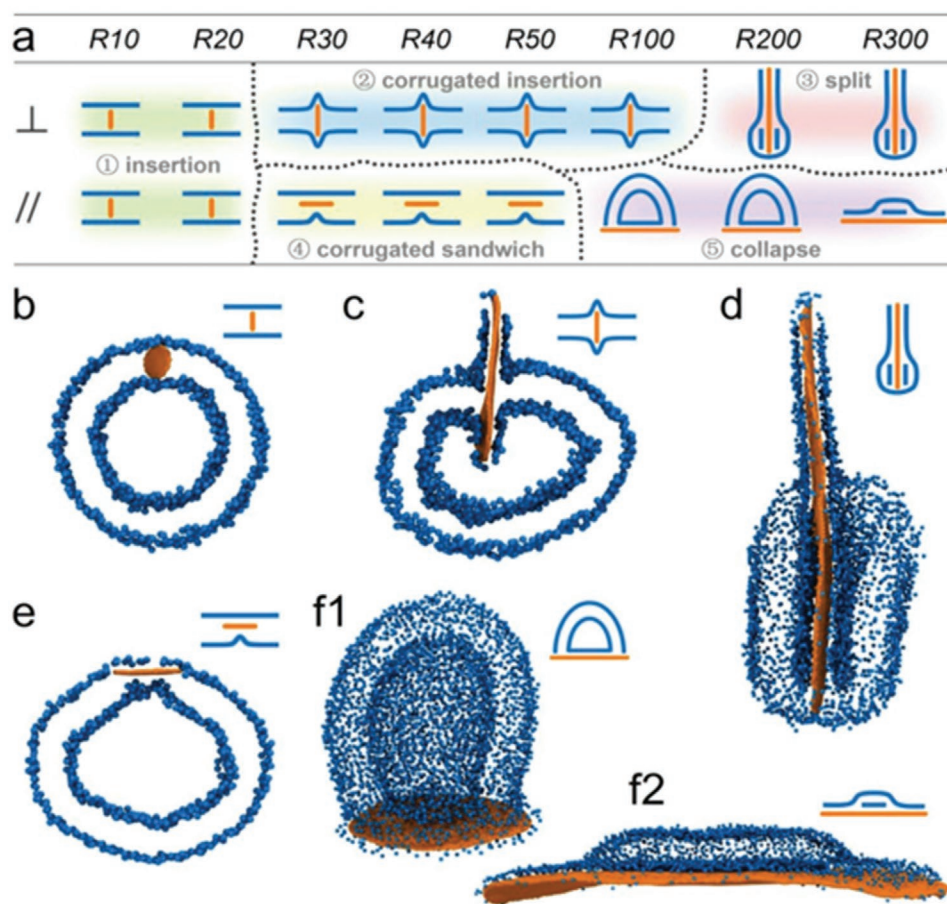
Figure 7. GMs-phospholipids interaction: other mode based on a liposome model. a) Interaction states of hydrophobic nanosheets and liposome varied over the size and initial orientation of nanosheets. b–f) Representative snapshots of models of b) R20⊥, c) R50⊥, d) R200⊥, e) R40 ∥, f1) R100∥, and f2) R300∥. Symbol ⊥ represents the perpendicular orientation, while symbol ∥ indicates the parallel orientation of nanosheet. R is the radius of the nanosheet. Reproduced with permission.[63] Copyright 2018, Wiley-VCH.

**ADVANCED
SCIENCE NEWS**
www.advancedsciencenews.com

**ADVANCED
MATERIALS
INTERFACES**
www.advmatinterfaces.de

toward the interior and eventually flip-fop into the inner leaflet of lipid bilayer. Nevertheless, the authors concluded that smaller nanosheets preferentially inserted perpendicularly into the lipid membrane, which might not be destructive to the liposome, but could have dramatic influence on the fluidity of the lipid membrane. Sheets larger than the liposome led to complete membrane deformation (e.g. lipid spread). Furthermore, multiple nanosheets exhibited similar behavior on the membrane compared to that of a single nanosheet, but an accumulated effect of aggregated nanosheets can be expected to cause a stronger impact on the lipid membrane. All in all, the interaction mechanisms were closely associated with the physiochemical properties of GMs and the simulation details. We believe that this work has set a good example for future studies to avoid conflicting results in this area.

3. Interaction Between Cholesterol and GMs

Cholesterol is a type of lipid that plays an essential role in adjusting membrane fluidity.[64] Moreover, cholesterol, together with sphingolipid and protein receptors, constitutes so-called lipid rafts, which are microdomains on cell membranes that regulate cell signaling.[65] The interaction between cholesterol and GMs thus has a high potential to affect cell signaling pathways. To date, only few reports attempted to understand such interaction. Two mechanisms on certain cell lines have been reported, which are cholesterol extraction and cholesterol oxidation.

3.1. Cholesterol Extraction

Zhang and coworkers, using dissipative dynamic simulations, demonstrated that single-layered graphene with an initial orientation perpendicular to the membrane was capable of continuously extracting cholesterol molecules from a cell membrane consisting of lipid, cholesterol, and protein receptors.[66] By contract, graphene oriented parallel to the membrane caused a local accumulation of cholesterol in the membrane patch interacting with graphene (**Figure 8**a). The hydrophobic interaction between graphene and cholesterol dominated the process of extraction. Computational models indicated that graphene had a tendency to attach to the surface of the cell membrane rather than penetrate into the membrane after the completion of extraction process, which was different to the previously discussed phospholipid extraction mode.[34] Nevertheless, the extraction of cholesterol also resulted in loss of membrane integrity, which might be another possible explanation for cytotoxicity of GMs.

Later in 2018, Kitko et al. offered experimental results in two eukaryotic cell lines: neurons and fibroblast NIH-3T3 cells to support this cholesterol extraction mode.[67] After culturing cells on graphene coated glass coverslips, the authors observed obviously increased cholesterol levels in the PMs of both cell types (Figure 8b). Meanwhile, graphene film used in this work showed minimum affinity to other common biomolecules on cell membranes (phospholipids, carbohydrates, and proteins). However, the reason behind the selective extraction of

cholesterol was not clear. Besides that, the authors also noticed a potentiation of neurotransmission and a promoted activation of P2Y receptor-mediated Ca^{2+} response in NIH-3T3 cells. According to the authors, such biological effects of graphene relied on its ability to recruit cholesterol as a mediator, since it is known that cholesterol participates in many signaling pathways. However, Kitko and coworkers could not clarify whether the abundant cholesterol attracted by graphene film came from other endogenous membranes (endoplasmic reticulum for example) or the culture media. To answer this question, a precise tracking of cholesterol transport would be required.

In line with previous studies, Bernabò and colleagues reported for the first time that GO nanosheets at low concentrations (0.5–1 µg mL^{-1}) could improve the fertilizing ability of spermatozoa from swine in vitro, via extracting cholesterol from cell membranes.[69] The authors proposed that the adsorption of cholesterol on the surface of GO decreased total concentration of cholesterol in the sperm cell, which increased the membrane fluidity and enhanced Ca^{2+} permeability. Consequently, sperm signaling function was positively adjusted, leading to a higher fertilization potential.

3.2. Cholesterol Oxidation

Mukherjee et al. identified that GO was able to directly oxidize cholesterol in neutrophils, leading to the disruption of lipid rafts and followed by a cascade of intracellular events that eventually activated a conserved anti-pathogen response: formation of neutrophil extracellular traps (NETs),[68] as shown in Figure 8c. In addition, GO-induced NETs release was size-dependent; large GO flakes had a stronger influence than the small flakes. With the assistance of electron microscopy, optical microscopy, and mass spectroscopy, the authors provided direct experimental proof for cholesterol oxidation. Moreover, they also claimed that adding a simple antioxidant could effectively prevent the oxidation of cholesterol by GO and reduce NET formation, which might be a promising strategy to reduce cytotoxicity of GO on neutrophils.

4. Interaction Between Membrane Proteins and GMs

Membrane proteins, especially integral membrane proteins, are preferable targets of numerous drugs due to their involvement in selective transport of many signals, molecules and ions between internal and external environments of cells. Several publications have documented that GMs could selectively bind to membrane receptors, such as toll-like receptors (TLRs),[70] aquaporin (AQP1),[71] integrin,[72] which thereby activated downstream signaling pathways. This opens additional routes for biological applications of GMs. Notably, none of these reports clarified questions such as: why GO had selectivity to only some certain membrane proteins, how exactly GO activated signaling pathways, or what specific motif of membrane proteins was bound to GMs. Hence, more efforts are necessary to uncover the detailed mechanism of interaction between GMs and membrane proteins.
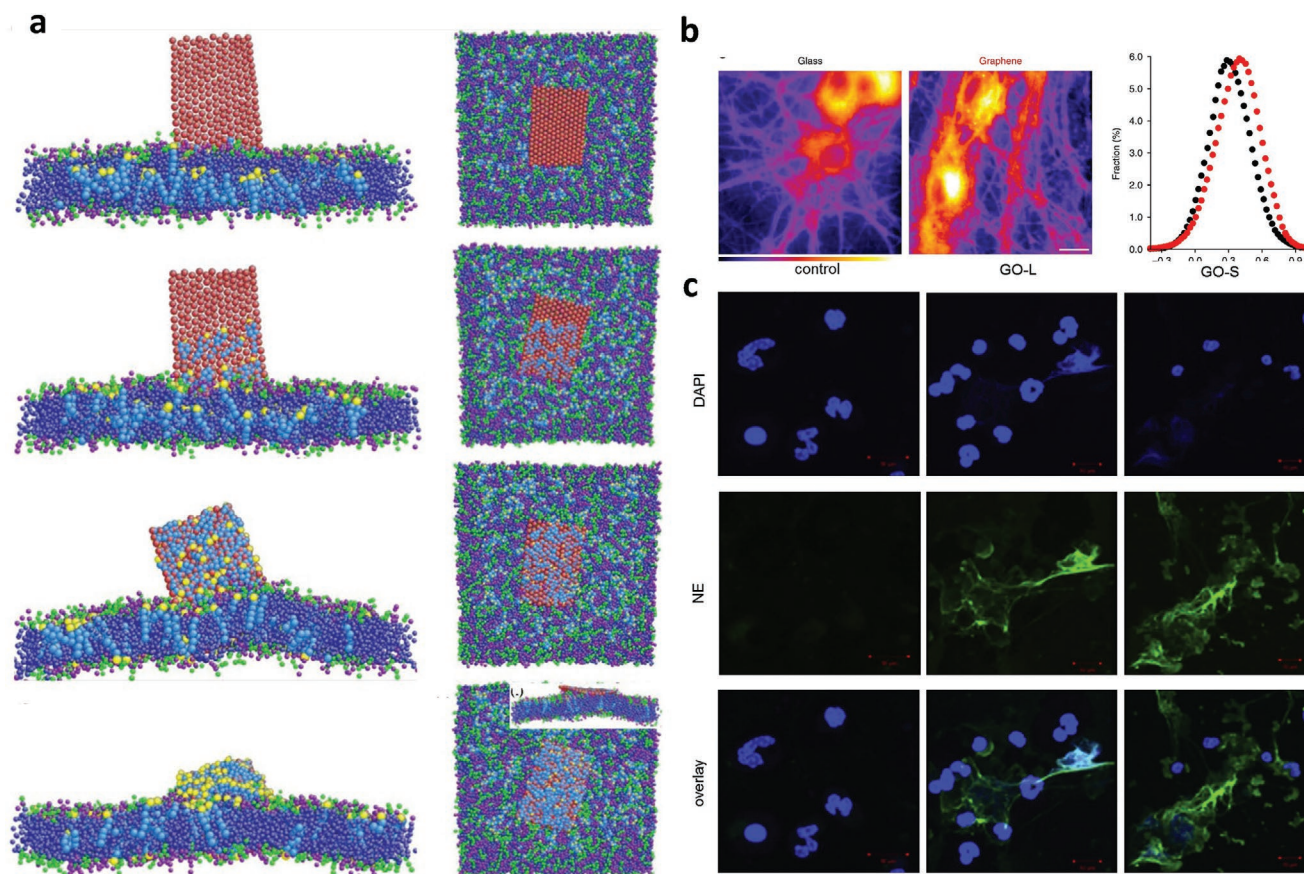
**ADVANCED
SCIENCE NEWS**

www.advancedsciencenews.com

**ADVANCED
MATERIALS
INTERFACES**

www.advmatinterfaces.de

Figure 8. GMs-cholesterol interaction: cholesterol extraction and oxidation. a) Representative trajectories of extraction of cholesterol from cell membrane by graphene sheet with a vertical orientation (left) and a horizontal orientation (right). The tails of lipid are displayed in blue while the heads of lipid are displayed in green. The tails of receptor are shown in blue while the heads of receptor are shown in purple. Light blue represents the tails of cholesterol while yellow represents the heads of cholesterol. The red sheet represents graphene. b) Generalized polarization (GP) images of living neurons on the surface of bare glass coverslips (black) and graphene coated glass (red) indicating the increased membrane cholesterol. Scale bar = 20 μm. The GP images is pseudo-colored: low GP value is shown in purple while high GP value is shown in light yellow. GP values range from −1 to 1. The increase of GP value indicates higher amount of cholesterol on the substrate. c) Confocal images of neutrophils incubated without (control) and with GO-L or GO-S (12.5 μg mL⁻¹, 2 h). Both neutrophil elastase and nuclear of cells were stained, where their false color was green and blue, respectively. Scale bar = 10 μm. a) Reproduced with permission.[66] Copyright 2016, American Chemical Society. b) Reproduced under the terms of the CC-BY 4.0 license.[67] Copyright 2018, The Authors, published by Springer Nature. c) Reproduced with permission.[68] Copyright 2017, Elsevier Inc.

4.1. Interaction with TLRs

Qu and coworkers observed necrosis of microphages after exposure of two microphage cell lines (J774A.1 and RAW 264.7) to GO. The interaction between GO and TLR4 was proven to be the major underlying mechanism for GO-induced necrosis.[70] On one hand, this interaction triggered secretion of proinflammatory cytokine tumor necrosis factor alpha (TNF-α), which is known to cause programmed necrosis of microphage. On the other hand, large number of ROS was generated as a consequence of GO-TLR4 interaction, which further promoted the necrotic process via oxidative stress. In addition, the internalization and intracellular accumulation of GO also contributed the cytotoxicity of GO by damaging cytoskeletal network on cell membrane. Hence, the authors proposed a synergistic effect to explain the underlying mechanism of GO-induced necrosis (**Figure 9**a).

In line with Qu's report, Ma et al. further attributed the cytotoxic mechanism of GO to its ability to generate significant

inflammatory responses. And GO-triggered inflammation showed a size-dependent feature.[73] According to Ma's results, large GO flakes (50–1300 nm) that adhered onto the cell membrane could activate TLRs and downstream NF-κB pathway both in J774A.1 cell and in mice. This was associated with enhanced M1 polarization, excretion of TNF-α and recruitment of immune cells. Conversely, small GO flakes (50–350 nm) stimulated less inflammation under the same experimental conditions. The suggested rationale was that easy permeation of smaller GO through the cell membrane resulted in their accumulation inside microphages. This depleted the pool of smaller GO flakes available for sticking onto the outer surface of the PM, where they could interact with the TLRs.

4.2. Interaction with AQP1

Apart from size effect, researchers also examined the effect of incubation time on GO's interaction with membrane proteins.
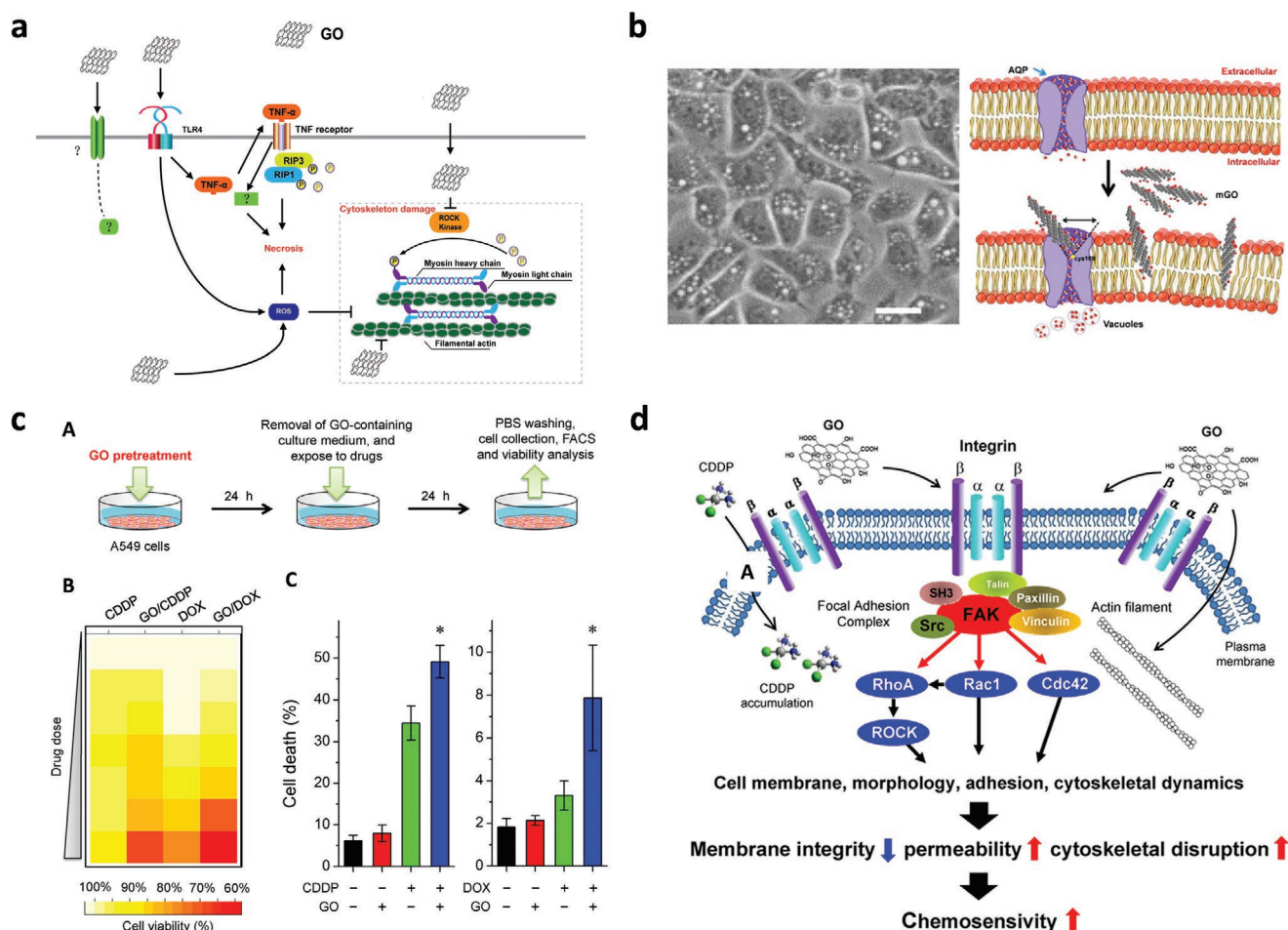
Figure 9. GMs-membrane proteins interaction: a) Schematic diagram illustrating the interaction of GO and TLR4 which induced production of TNF-α and thereby activated programmed necrosis of macrophages. The oxidative stress and cytoskeletal disruption caused by intracellular accumulation of GO were also elucidated. b) Left: TEM images of MCF-7 cells treated with mGO (50 μg mL^{-1}) for 6 h. Scale bar = 10 μm. Right: schematic diagram of interaction between micro-sized GO and AQPs which led to increase of membrane permeability. c) The sensitization of A549 cells to anticancer drugs DOX and cisplatin (CDDP) by GO treatment. c-A) Schematic illustration of the experiment design: A549 cells were pretreated with GO at 10 μg mL^{-1} for 24 h, followed by PBS washing, and were then exposed to CDDP or DOX at certain concentrations for another 24 h. c-B) Heatmap of cell viability for free drugs treated cells and GO pretreated cells after drugs exposure. The concentrations of CDDP were set from 1 to 50 μM, while concentration rang for DOX was 0.01–4 μM. c-C) Fluorescence-activated cell sorting analysis for quantification of cell viability. The concentration of CDDP and DOX was 20 and 0.1 μM, respectively. d) Schematic illustration of molecular basis underlying GO-enhanced drug uptake. The interaction of GO and integrin activated subsequent integrin-FAK-Rho-ROCK signaling pathway, leading to compromised membrane and cytoskeleton. a) Reproduced with permission.[70] Copyright 2013, American Chemical Society. b) Reproduced with permission.[71] Copyright 2015, American Chemical Society. c,d) Reproduced with permission.[72] Copyright 2017, American Chemical Society.

Wu et al. claimed that within a short incubation time (less than 24 h), micrometer-sized GO (mGO, 0.5–3 μm) interacted with AQP1, a water transport channel. The hydrophobic interaction of GO with AQP1 on the extracellular side induced the formation of vacuoles in cytoplasm and enhanced membrane permeability, without damaging membrane integrity or exhibiting any obvious cytotoxicity (Figure 9b).[71] Typically, the increase of membrane permeability facilitated cellular uptake of small molecules, for example, propidium iodide (PI), whereas macromolecules, such as proteins were still not able to penetrate the cell membrane. The authors found out that this vacuolization phenomenon was universal in several cell lines that had a high AQP1 expression level, including MCF-7, human erythrocytes, A549, AGS, and SGC7901. Interestingly, the size and number of

vacuoles could decrease or even vanish after prolonging incubation time. Conversely, nanometer-sized GO failed to induce vacuolization, no matter how long they were exposed to cells. This is most likely due to cellular uptake, which was in line with previous reports.[73] Later, Sui et al. confirmed this mGO-induced improvement of cell permeability by quantifying cellular uptake of cisplatin (CDDP) (a chemotherapeutic agent used for cancer therapy).[74] Compared with untreated MCF-7 cells, mGO treated cells exhibited one-fold higher cisplatin accumulation inside cells. This highlights the potential of mGO as an effective assistant agent for improving chemotherapy performance of small molecular anticancer drugs, as well as overcoming drug resistance. Additionally, GQDs with an average size of 40 nm also increased cellular and nuclear uptake of cisplatin

**ADVANCED
SCIENCE NEWS**

www.advancedsciencenews.com

**ADVANCED
MATERIALS
INTERFACES**

www.advmatinterfaces.de

due to improved cell membrane permeability, according to Sui et al. But neither vacuolization nor any other molecular mechanism was reported. Hence the report by Sui et al.[74] did not support the hypothesis of Wu et al.,[71] but rather fueled an ongoing debate regarding the size effect in GMs-AQP1 interaction.

4.3. Interaction with Integrin

Zhu and coworkers discovered that nano-sized GO (100–300 nm) could also boost the uptake of chemotherapeutic drugs doxorubicin (DOX) and cisplatin inside A549, A49 renal, and PC3 prostate cancer cells (Figure 9c).[72] As evidenced by PI staining, TO-PRO-3 staining, lactate dehydrogenase assay and membrane topography analysis, the authors concluded that GO-treated cancer cells featured a loss of membrane integrity and an impaired actin cytoskeleton network. This had negligible influence on cell viability but was beneficial for sensitizing cancer cells for chemotherapeutic agents. Molecular basis underling cellular effects of GO was related to the activation of the integrin–FAK–Rho–ROCK pathway, which caused a lower integrin expression on the cell membrane. The whole process was trigged by GO-integrin interaction (Figure 9d). Since integrin was crucial for maintaining the cell membrane and cytoskeleton, suppressing the expression of integrin could explain the enhanced cell permeability. This dynamic mechanism was not fully in agreement with previous results,[71,74] although similar outcomes were achieved, specifically: enhancement of membrane permeability and influx of anticancer drugs. Clearly, further investigation is needed to settle the ongoing debate.

4.4. Guidelines for Biomedical Applications of GMs

In previous sections, we have summarized the interactions of GMs with well-known components of biological membranes. The following part will focus on offering guidelines for more effective and safer biomedical applications based on what has been learned from the known underlying mechanisms. Specifically, we will discuss how to modulate the performance of GMs in bacterial killing and cancer therapy.

4.5. Enhancing Antibacterial Activity

Mechanical damage, oxidative stress, and wrapping have been accepted as the three main antibacterial mechanisms.[75] From a molecular perspective, interaction between GMs and phospholipids can provide support for each mechanism, as displayed in **Scheme 1**. Briefly, graphene insertion, lipid extraction, and pore formation are known to result in mechanical damage on cell membranes, while lipid peroxidation and ET support the well-known oxidative stress mechanism. The masking mode could be the underlying basis of the wrapping mechanism. As discussed above, antibacterial activity of GMs could be dramatically affected by their structural characteristics, including size, surface roughness, aggregation, orientation, and oxidative level.[76] Due to inconsistent experimental methodologies, it is
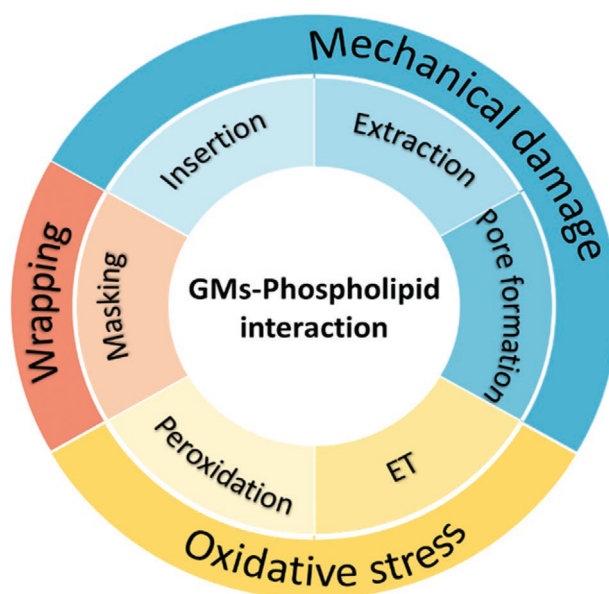
Scheme 1. Schematic diagram elucidating the three major antibacterial mechanisms and their underlying molecular basis.

still challenging to establish a predictable structure-property-bioactivity relationship.[77] Nevertheless, some general rules can be applied to enhance the antibacterial performance of GMs with the gained knowledge on molecular mechanisms in recent years.

In general, larger size, sharper edge, and aggregation are beneficial for inserting/cutting mode, lipid extraction mode and pore formation mode, leading to stronger membrane destabilization.[78] The wrapping or masking mechanism also requires large lateral size of the GMs, specifically micrometer-sized GMs.[51] In contrast, basal plane and oxidative level of GMs play crucial roles for ROS-dependent oxidative stress since they determine lipid peroxidation. Current results support that the higher the oxidative level of GMs, the more cytotoxicity can be achieved.[56] Small-sized GMs usually accelerate oxidative stress owing to the fact that the defect density increases with the decline of the GMs' size.[78] ET-based damage can be promoted significantly when coating GMs on conductive substrates, which may provide a useful strategy for developing efficient antibacterial coatings.[60] The remaining open question is the relationship between toxicity and the size of GMs. Further studies should focus on identifying the dominant antibacterial mechanism, in order to guide the size selection of GMs to be used in antibacterial applications.

The orientation of GMs could also be tailored for fabricating superior antibacterial coatings.[79] Magnetic field was used to tune the orientation of GMs.[80] Developing chemical vapor deposition method with specific growth parameters was reported as another effective way for controlling the alignment of GMs.[81] Several published papers have observed that vertically aligned GMs were significantly more lethal for bacterial cells than randomly orientated GMs.[82] This might arise from the synergistic effect of increased physical puncturing of cell membranes and more effective electron transfer since cell membrane and vertical GMs had better contact with each other.[38a]

A very recent study indicated experimentally and theoretically that covalent bounding of silver nanoparticles (AgNPs) to cyanographene (GCN) exhibited excellent antibacterial activity against multidrug resistant strains. The bonding of AgNPs caused more severe membrane perturbation compared with bare GCN or AgNPs, owing to its stronger interaction with the bacterial membrane.[83] This may offer another method for designing GMs-based antibiotic agents with desired efficiency.

Besides tailoring the structural properties of GMs, establishing proper experimental methods also has a significant impact on bacterial killing efficiency. For instance, the exposure of GMs in solution to bacterial cells in the planktonic state could exhibit higher antibacterial activity compared with the efficiency of killing biofilms. This is because bacteria inside biofilms have less opportunity to come into contact with GMs due to the protection of the extracellular matrix. However, in real biomedical applications, GMs often encounter colonies of bacterial cells and biofilms. Hence, the method for antimicrobial assessment should be chosen carefully, depending on the proposed type of biomedical application. Furthermore, quantitative methods should be prioritized to determine the number of live/dead cells, rather than employing qualitative assessment, so as to standardize the antibacterial efficiency of GMs.

4.6. Reducing Cytotoxicity for Mammalian Cells

To apply GMs as biomedicine, the cytotoxicity of GMs for mammalian cells must be eliminated.[84] The above-mentioned interactions of GMs with phospholipids, cholesterol, and membrane proteins generally induce membrane damage or oxidative stress, which eventually result in declined cell viability with the increase of incubation time or concentration.[85] Reducing the GMs-membrane interaction by shielding GMs with a protein corona may be a feasible solution.[86] As demonstrated by experiments, protein (FBS) coated GO had almost no cytotoxicity for A549 cells at high concentration.[87] Moreover, hemolytic activity of GO could be greatly reduced using this protein corona effect. Theoretical model revealed that with the surface of GO being occupied by proteins, the available surface area of GO reduced and the steric effect increased. This in turn weakened the physical interaction between GO and the membrane, more specifically, insertion mode and lipid extraction mode.[88] However, whether the protein corona has any influence on the interaction between GMs and the other membrane components, such as cholesterol and membrane proteins, still remains to be investigated.

In addition to a protein corona, various biocompatible small molecules or polymers have been shown to be useful for reducing cytotoxicity of GMs.[89] Though this approach appears to be promising, the underlying mechanism of how such a coating mitigates cytotoxicity of GMs has not been investigated. In future, more attention should be paid to studying mechanisms.

Adding antioxidants was reported to be effective for mitigating cholesterol oxidation on neutrophils.[68] Along the same lines, blocking certain signaling pathways (e.g., TLR4) using selective inhibitors might completely preclude cell death

induced by GO.[70] Additionally, single layered GO exhibited stronger cell proliferation and higher ROS generation than four layered GO, which emphasized the importance of the number of layers of GMs in toxicology.[90] These preliminary results need to be verified in more cell lines, and their mechanism of action should be explained before they can be generally recommended for mitigating cytotoxicity.

Impurity and instability of GMs in aqueous solution might contribute to their safety risks as well.[91] Ali-Boucetta et al. illustrated that GO with high purity and good dispersibility exhibited minimum cytotoxic responses for A549 cells at a concentration of 100 µg mL⁻¹.[92] After a 7-day exposure, no inflammation or granuloma formation was observed in a mouse model that was injected with GO at a dose of 50 µg mL⁻¹. This suggested that a precise control of quality and purity of GMs was more crucial than initially thought, and could lead to more reliable and reproducible results.[93]

4.7. Improving Selectivity for Cancer Cells

Functionalization of GMs with cancer-cell-targeting molecules, for instance, folic acid,[94] peptide nucleic acids,[95] DNA[96] has been widely applied for GMs-based selective cancer treatment. Meanwhile, inspired by the ability of GMs to activate transport pathways via interaction with membrane proteins (e.g. AQP1), researchers have designed an effective and convenient platform for improved cancer chemotherapy.[71] Indeed, increasing membrane permeability and facilitating drug influx inside cancer cells can be a valuable strategy for cancer therapy and even for overcoming drug resistance if it is tumor targeted. However, based on current knowledge, GMs could be expected to activate various signaling pathways in both normal and cancer cell lines. Size may affect GMs-membrane protein interaction, but the relationship between size and selectivity is still unclear. Promoting the selectivity for membrane proteins that are overexpressed on cancer cells will definitely be beneficial for the application of GMs in cancer therapy. But such optimization can only become possible once the interaction mechanisms between GMs and proteins are better understood.

5. Conclusions

In this review, we have summarized the molecular mechanisms of how GMs interact with major components on biological membranes, more specifically, phospholipids, cholesterol, and membrane proteins. Based on those, we proposed some general guidelines for modulating the biological performance of GMs in the area of antibacterial activity and cancer therapy. However, we are still far from fully understanding the relationship between cytotoxicity and the intrinsic properties of GMs (e.g., surface area, thickness, aggregation). Several fundamental problems must be solved before drawing any universal conclusions.

The most crucial of these challenges is the absence of strict standards for quality evaluation of GMs and methodologies used in subsequent biological experiments. For instance, many publications emphasized the significance of the size effect in

the biological response of GMs. They all used the same term "micro-sized GO", but the actual size of GMs they adapted ranged from tens of nanometers to several micrometers in different studies. In addition to setting experimental standards for GMs, theoretical simulation regarding GMs and their interaction with biological membranes should also be standardized. Here, model of GMs and lipid membrane, force field (polarizable or nonpolarizable), convergence, solvent model, counterions, mixing rules, etc. are critical parameters that may significantly affect the results of molecular simulations.[97] To settle the ongoing debates, it is important to establish both experimental and theoretical standards in this area.

The second issue concerns the insufficient understanding of mechanisms governing the interaction of GMs with cells. Although a majority of current research focuses on the antibacterial effects, GMs also have been reported to induce membrane damage on fungi,[28b] virus,[98] yeast,[99] algae,[100] cyanobacteria.[100] It was illustrated that GO with a low degree of oxidation could act as a nano-blade and cause mechanical damage on cell membranes of cyanobacterium and algae,[100] which was widely used to explain the antibacterial activity of GO. Some studies have evaluated toxicity of GMs on plant cells (e.g. oxidative stress and drought stress), but molecular mechanisms are still lacking.[101] Taking the diversity of biological membranes into consideration, it is not accurate to explain the toxicity of GMs for fungi or algae by drawing on the knowledge gathered about bacterial cells. In addition to the cell membrane, other components of the cellular envelope such as the cell wall may influence the interaction with GMs. Indeed, in bacteria, the cell wall composed of peptidoglycans and polysaccharides is the first surface the GMs will encounter, before they can interact with the cellular membrane. Yet there is no experimentally derived conclusive information on how GMs interact with the cell wall. In addition to that, GMs accumulated inside cells could potentially interact with crucial intracellular molecules (proteins, ATP, DNA/RNA, et al.) and organelles (mitochondria) via hydrogen bonding, π–π stacking, or electrostatic adsorption. This could eventually cause intracellular stress and induce cell killing, which should be considered as antibacterial mechanisms as well. In future studies, it is important to experimentally discriminate between different antibacterial mechanisms and identify the relative contributions of each mechanism to the overall bactericidal effect.

Finally, the theoretical models and experimental data need to become more connected and consistent with each other. For instance, the physiochemical properties we discussed above should be taken into account when building graphene models in simulation. The composition, fluidity, and dynamic structure of cell membranes have to be considered thoroughly for more precise insights into GMs-membrane interaction. However, it is not uncommon that some researchers use GO in actual experiments but use PG as a theoretical model in their computational simulations. Due to large differences in material properties, no reliable conclusions can be drawn from such comparisons.

To sum up, investigation of molecular mechanisms and standardization of materials and experimental methods are the most logical future steps in the field of GMs-based biomedical applications.

[1] V. C. Sanchez, A. Jachak, R. H. Hurt, A. B. Kane, *Chem. Res. Toxicol.* **2012**, *25*, 15.

[2] Z. Tu, G. Guday, M. Adeli, R. Haag, *Adv. Mater.* **2018**, *30*, 1706709.

[3] G. Reina, J. M. González-Domínguez, A. Criado, E. Vázquez, A. Bianco, M. Prato, *Chem. Soc. Rev.* **2017**, *46*, 4400.

[4] S. M. Mousavi, F. W. Low, S. A. Hashemi, N. A. Samsudin, M. Shakeri, Y. Yusoff, M. Rahsepar, C. W. Lai, A. Babapoor, S. Soroshnia, S. M. Goh, S. K. Tiong, N. Amin, *RSC Adv.* **2020**, *10*, 12851.

[5] Y. Qu, F. He, C. Yu, X. Liang, D. Liang, L. Ma, Q. Zhang, J. Lv, J. Wu, *Mater. Sci. Eng., C* **2018**, *90*, 764.

[6] A. Deb, N. G. Andrews, V. Raghavan, *Int. J. Biol. Macromol.* **2018**, *113*, 515.

[7] J. Chu, P. Shi, W. Yan, J. Fu, Z. Yang, C. He, X. Deng, H. Liu, *Nanoscale* **2018**, *10*, 9547.

[8] R. Lima-Sousa, D. de Melo-Diogo, C. G. Alves, E. C. Costa, P. Ferreira, R. O. Louro, I. J. Correia, *Carbohydr. Polym.* **2018**, *200*, 93.

[9] Z. Wang, L. Colombi Ciacchi, G. Wei, *Appl. Sci.* **2017**, *7*, 1175.

[10] C. Cheng, S. Li, A. Thomas, N. A. Kotov, R. Haag, *Chem. Rev.* **2017**, *117*, 1826.

[11] D. Bitounis, H. Ali-Boucetta, B. H. Hong, D.-H. Min, K. Kostarelos, *Adv. Mater.* **2013**, *25*, 2258.

[12] H. E. Karahan, C. Wiraja, C. Xu, J. Wei, Y. Wang, L. Wang, F. Liu, Y. Chen, *Adv. Healthcare Mater.* **2018**, *7*, 1701406.

[13] Z. Gu, S. Zhu, L. Yan, F. Zhao, Y. Zhao, *Adv. Mater.* **2019**, *31*, 1800662.

[14] a) T.-H. Kim, D. Lee, J.-W. Choi, *Biosens. Bioelectron.* **2017**, *94*, 485; b) J. Luo, X. Zhao, J. Wu, H. D. Jang, H. H. Kung, J. Huang, *J. Phys. Chem. Lett.* **2012**, *3*, 1824.

[15] Q. Zhang, Z. Wu, N. Li, Y. Pu, B. Wang, T. Zhang, J. Tao, *Mater. Sci. Eng., C* **2017**, *77*, 1363.

[16] a) A. Piperno, A. Scala, A. Mazzaglia, G. Neri, R. Pennisi, M. T. Sciortino, G. Grassi, *Int. J. Mol. Sci.* **2018**, *19*, 3365; b) R. Rauti, N. Lozano, V. León, D. Scaini, M. Musto, I. Rago, F. P. Ulloa Severino, A. Fabbro, L. Casalis, E. Vázquez, K. Kostarelos, M. Prato, L. Ballerini, *ACS Nano* **2016**, *10*, 4459; c) L. Golubewa, H. Rehman, T. Kulahava, R. Karpicz, M. Baah, T. Kaplas, A. Shah, S. Malykhin, A. Obraztsov, D. Rutkauskas, M. Jankunec, I. Matulaitienė, A. Selskis, A. Denisov, Y. Svirko, P. Kuzhir, *Sensors* **2020**, *20*, 5028.

[17] a) H. Ji, H. Sun, X. Qu, *Adv. Drug Delivery Rev.* **2016**, *105*, 176; b) K. Yang, Y. Li, X. Tan, R. Peng, Z. Liu, *Small* **2013**, *9*, 1492.

[18] K. P. Loh, D. Ho, G. N. C. Chiu, D. T. Leong, G. Pastorin, E. K.-H. Chow, *Adv. Mater.* **2018**, *30*, 1802368.

[19] M. Verdanova, B. Rezek, A. Broz, E. Ukraintsev, O. Babchenko, A. Artemenko, T. Izak, A. Kromka, M. Kalbac, M. H. Kalbacova, *Small* **2016**, *12*, 2499.

[20] W. C. Lee, C. H. Y. X. Lim, H. Shi, L. A. L. Tang, Y. Wang, C. T. Lim, K. P. Loh, *ACS Nano* **2011**, *5*, 7334.

[21] P. K. C. Kenry, K. P. Loh, C. T. Lim, *ACS Nano* **2016**, *10*, 3424.

[22] a) M. Amrollahi-Sharifabadi, M. K. Koohi, E. Zayerzadeh, M. H. Hablolvarid, J. Hassan, A. M. Seifalian, *Int. J. Nanomed.* **2018**, *13*, 4757; b) K. Yang, J. Wan, S. Zhang, Y. Zhang, S.-T. Lee, Z. Liu, *ACS Nano* **2011**, *5*, 516; c) K. Yang, H. Gong, X. Shi, J. Wan, Y. Zhang, Z. Liu, *Biomaterials* **2013**, *34*, 2787.

[23] X. Hu, Q. Zhou, *Chem. Rev.* **2013**, *113*, 3815.

[24] K. Ghosal, K. Sarkar, *ACS Biomater. Sci. Eng.* **2018**, *4*, 2653.

[25] C. A. Amadei, P. Arribas, C. D. Vecitis, *Carbon* **2018**, *133*, 398.

[26] a) A. Bianco, H.-M. Cheng, T. Enoki, Y. Gogotsi, R. H. Hurt, N. Koratkar, T. Kyotani, M. Monthioux, C. R. Park, J. M. D. Tascon, J. Zhang, *Carbon* **2013**, *65*, 1; b) P. Wick, A. E. Louw-Gaume, M. Kucki, H. F. Krug, K. Kostarelos, B. Fadeel, K. A. Dawson, A. Salvati, E. Vázquez, L. Ballerini, M. Tretiach, F. Benfenati, E. Flahaut, L. Gauthier, M. Prato, A. Bianco, *Angew. Chem., Int. Ed.* **2014**, *53*, 7714.

[27] G. van Meer, D. R. Voelker, G. W. Feigenson, *Nat. Rev. Mol. Cell Biol.* **2008**, *9*, 112.

[28] a) J. Ruiz-Herrera, L. Ortiz-Castellanos, *FEMS Yeast Res.* **2010**, *10*, 225; b) J. Chen, H. Peng, X. Wang, F. Shao, Z. Yuan, H. Han, *Nanoscale* **2014**, *6*, 1879.

[29] L. Brown, J. M. Wolf, R. Prados-Rosales, A. Casadevall, *Nat. Rev. Microbiol.* **2015**, *13*, 620.

[30] a) E. Yamamoto, T. Akimoto, A. C. Kalli, K. Yasuoka, M. S. P. Sansom, *Sci. Adv.* **2017**, *3*, e1601871; b) S.-H. Kim, J. Turnbull, S. Guimond, *J. Endocrinol.* **2011**, *209*, 139; c) P. Chen, H. Yue, X. Zhai, Z. Huang, G.-H. Ma, W. Wei, L.-T. Yan, *Sci. Adv.* **2019**, *5*, eaaw3192.

[31] P. Chen, L.-T. Yan, *J. Mater. Chem. B* **2017**, *5*, 4290.

[32] a) Q. Xin, H. Shah, A. Nawaz, W. Xie, M. Z. Akram, A. Batool, L. Tian, S. U. Jan, R. Boddula, B. Guo, Q. Liu, J. R. Gong, *Adv. Mater.* **2019**, *31*, 1804838; b) M. D. Rojas-Andrade, G. Chata, D. Rouholiman, J. Liu, C. Saltikov, S. Chen, *Nanoscale* **2017**, *9*, 994; c) S. Begum, A. Pramanik, D. Davis, S. Patibandla, K. Gates, Y. Gao, P. C. Ray, *ACS Omega* **2020**, *5*, 3116; d) X. Zou, L. Zhang, Z. Wang, Y. Luo, *J. Am. Chem. Soc.* **2016**, *138*, 2064.

[33] O. Akhavan, E. Ghaderi, *ACS Nano* **2010**, *4*, 5731.

[34] Y. Tu, M. Lv, P. Xiu, T. Huynh, M. Zhang, M. Castelli, Z. Liu, Q. Huang, C. Fan, H. Fang, R. Zhou, *Nat. Nanotechnol.* **2013**, *8*, 594.

[35] Y. Chen, L. Zhou, J. Wang, X. Liu, H. Lu, L. Liu, F. Lv, S. Wang, *ACS Appl. Mater. Interfaces* **2018**, *10*, 27555.

[36] D. M. Engelman, *Nature* **2005**, *438*, 578.

[37] W. Hu, C. Peng, W. Luo, M. Lv, X. Li, D. Li, Q. Huang, C. Fan, *ACS Nano* **2010**, *4*, 4317.

[38] a) X. Lu, X. Feng, J. R. Werber, C. Chu, I. Zucker, J.-H. Kim, C. O. Osuji, M. Elimelech, *Proc. Natl. Acad. Sci. U. S. A.* **2017**, *114*, E9793; b) S. Pandit, Z. Cao, V. R. S. S. Mokkapati, E. Celauro, A. Yurgens, M. Lovmar, F. Westerlund, J. Sun, I. Mijakovic, *Adv. Mater. Interfaces* **2018**, *5*, 1701331.

[39] a) J. D. Mangadlao, C. M. Santos, M. J. L. Felipe, A. C. C. de Leon, D. F. Rodrigues, R. C. Advincula, *Chem. Commun.* **2015**, *51*, 2886; b) L. Hui, J.-G. Piao, J. Auletta, K. Hu, Y. Zhu, T. Meyer, H. Liu, L. Yang, *ACS Appl. Mater. Interfaces* **2014**, *6*, 13183.

[40] A. V. Titov, P. Král, R. Pearson, *ACS Nano* **2010**, *4*, 229.

[41] Y. Li, H. Yuan, A. von dem Bussche, M. Creighton, R. H. Hurt, A. B. Kane, H. Gao, *Proc. Natl. Acad. Sci. USA* **2013**, *110*, 12295.

[42] R. Guo, J. Mao, L.-T. Yan, *Biomaterials* **2013**, *34*, 4296.

[43] X. Yi, H. Gao, *Nanoscale* **2015**, *7*, 5457.

[44] J. Wang, Y. Wei, X. Shi, H. Gao, *RSC Adv.* **2013**, *3*, 15776.

[45] B. Luan, T. Huynh, R. Zhou, *Nanoscale* **2016**, *8*, 5750.

[46] L. Wu, L. Zeng, X. Jiang, *J. Am. Chem. Soc.* **2015**, *137*, 10052.

[47] X. Zhang, F. Cao, L. Wu, X. Jiang, *Langmuir* **2019**, *35*, 14098.

[48] V. T. H. Pham, V. K. Truong, M. D. J. Quinn, S. M. Notley, Y. Guo, V. A. Baulin, M. Al Kobaisi, R. J. Crawford, E. P. Ivanova, *ACS Nano* **2015**, *9*, 8458.

[49] G. Duan, Y. Zhang, B. Luan, J. K. Weber, R. W. Zhou, Z. Yang, L. Zhao, J. Xu, J. Luo, R. Zhou, *Sci. Rep.* **2017**, *7*, 42767.

[50] J. Chen, G. Zhou, L. Chen, Y. Wang, X. Wang, S. Zeng, *J. Phys. Chem. C* **2016**, *120*, 6225.

[51] S. Liu, M. Hu, T. H. Zeng, R. Wu, R. Jiang, J. Wei, L. Wang, J. Kong, Y. Chen, *Langmuir* **2012**, *28*, 12364.

[52] M. Dallavalle, M. Calvaresi, A. Bottoni, M. Melle-Franco, F. Zerbetto, *ACS Appl. Mater. Interfaces* **2015**, *7*, 4406.

[53] N. Willems, A. Urtizberea, A. F. Verre, M. Iliut, M. Lelimousin, M. Hirtz, A. Vijayaraghavan, M. S. P. Sansom, *ACS Nano* **2017**, *11*, 1613.

[54] J. Russier, E. Treossi, A. Scarsi, F. Perrozzi, H. Dumortier, L. Ottaviano, M. Meneghetti, V. Palermo, A. Bianco, *Nanoscale* **2013**, *5*, 11234.

[55] M. Hirtz, A. Oikonomou, T. Georgiou, H. Fuchs, A. Vijayaraghavan, *Nat. Commun.* **2013**, *4*, 2591.

[56] R. Li, L. M. Guiney, C. H. Chang, N. D. Mansukhani, Z. Ji, X. Wang, Y.-P. Liao, W. Jiang, B. Sun, M. C. Hersam, A. E. Nel, T. Xia, *ACS Nano* **2018**, *12*, 1390.

[57] R. Li, Z. Ji, C. H. Chang, D. R. Dunphy, X. Cai, H. Meng, H. Zhang, B. Sun, X. Wang, J. Dong, S. Lin, M. Wang, Y.-P. Liao, C. J. Brinker, A. Nel, T. Xia, *ACS Nano* **2014**, *8*, 1771.

[58] K. Krishnamoorthy, M. Veerapandian, L.-H. Zhang, K. Yun, S. J. Kim, *J. Phys. Chem. C* **2012**, *116*, 17280.

[59] Z. Komeily-Nia, L.-T. Qu, J.-L. Li, *Small Sci.* **2021**, *1*, 2000026.

[60] J. Li, G. Wang, H. Zhu, M. Zhang, X. Zheng, Z. Di, X. Liu, X. Wang, *Sci. Rep.* **2014**, *4*, 4359.

[61] G. Wang, K. Tang, Z. Meng, P. Liu, S. Mo, B. Mehrjou, H. Wang, X. Liu, Z. Wu, P. K. Chu, *Adv. Mater.* **2020**, *32*, 2003616.

[62] S. Liu, T. H. Zeng, M. Hofmann, E. Burcombe, J. Wei, R. Jiang, J. Kong, Y. Chen, *ACS Nano* **2011**, *5*, 6971.

[63] Z. Li, Y. Zhang, J. Ma, Q. Meng, J. Fan, *Small* **2019**, *15*, 1804992.

[64] a) P. L. Yeagle, *Biochim. Biophys. Acta, Biomembr.* **1985**, *822*, 267; b) P. L. Yeagle, *Biochimie* **1991**, *73*, 1303.

[65] D. Lingwood, K. Simons, *Science* **2010**, *327*, 46.

[66] L. Zhang, B. Xu, X. Wang, *J. Phys. Chem. B* **2016**, *120*, 957.

[67] K. E. Kitko, T. Hong, R. M. Lazarenko, D. Ying, Y.-Q. Xu, Q. Zhang, *Nat. Commun.* **2018**, *9*, 796.

[68] S. P. Mukherjee, B. Lazzaretto, K. Hultenby, L. Newman, A. F. Rodrigues, N. Lozano, K. Kostarelos, P. Malmberg, B. Fadeel, *Chem* **2018**, *4*, 334.

[69] N. Bernabò, J. Machado-Simoes, L. Valbonetti, M. Ramal-Sanchez, G. Capacchietti, A. Fontana, R. Zappacosta, P. Palestini, L. Botto, M. Marchisio, P. Lanuti, M. Ciulla, A. Di Stefano, E. Fioroni, M. Spina, B. Barboni, *Sci. Rep.* **2019**, *9*, 8155.

[70] G. Qu, S. Liu, S. Zhang, L. Wang, X. Wang, B. Sun, N. Yin, X. Gao, T. Xia, J.-J. Chen, G.-B. Jiang, *ACS Nano* **2013**, *7*, 5732.

[71] C. Wu, C. Wang, J. Zheng, C. Luo, Y. Li, S. Guo, J. Zhang, *ACS Nano* **2015**, *9*, 7913.

[72] J. Zhu, M. Xu, M. Gao, Z. Zhang, Y. Xu, T. Xia, S. Liu, *ACS Nano* **2017**, *11*, 2637.

[73] J. Ma, R. Liu, X. Wang, Q. Liu, Y. Chen, R. P. Valle, Y. Y. Zuo, T. Xia, S. Liu, *ACS Nano* **2015**, *9*, 10498.

[74] X. Sui, C. Luo, C. Wang, F. Zhang, J. Zhang, S. Guo, *Nanomedicine* **2016**, *12*, 1997.

[75] X. Zeng, G. Wang, Y. Liu, X. Zhang, *Environ. Sci.: Nano* **2017**, *4*, 2248.

[76] W. Han, Z. Wu, Y. Li, Y. Wang, *Chem. Eng. J.* **2019**, *358*, 1022.

[77] A. C. Barrios, Y. Wang, L. M. Gilbertson, F. Perreault, *Environ. Sci. Technol.* **2019**, *53*, 14679.

[78] F. Perreault, A. F. de Faria, S. Nejati, M. Elimelech, *ACS Nano* **2015**, *9*, 7226.

[79] W. Wei, J. Li, Z. Liu, Y. Deng, D. Chen, P. Gu, G. Wang, X. Fan, *J. Mater. Chem. B* **2020**, *8*, 6069.

[80] K. Zheng, K. Li, T.-H. Chang, J. Xie, P.-Y. Chen, *Adv. Funct. Mater.* **2019**, *29*, 1904603.

[81] W. Zheng, X. Zhao, W. Fu, *ACS Appl. Mater. Interfaces* **2021**, *13*, 9561.

[82] S. Pandit, K. Gaska, V. R. S. S. Mokkapati, E. Celauro, A. Derouiche, S. Forsberg, M. Svensson, R. Kádár, I. Mijakovic, *Small* **2020**, *16*, 1904756.

[83] D. Panáček, L. Hochvaldová, A. Bakandritsos, T. Malina, M. Langer, J. Belza, J. Martincová, R. Večeřová, P. Lazar, K. Poláková, J. Kolařík, L. Válková, M. Kolář, M. Otyepka, A. Panáček, R. Zbořil, *Adv. Sci.* **2021**, *8*, 2003090.

[84] F. Xiaoli, C. Qiyue, G. Weihong, Z. Yaqing, H. Chen, W. Junrong, S. Longquan, *Arch. Toxicol.* **2020**, *94*, 1915.

[85] V. Gies, S. Zou, *Toxicol. Res.* **2017**, *7*, 93.

[86] M. Papi, M. C. Lauriola, V. Palmieri, G. Ciasca, G. Maulucci, M. De Spirito, *RSC Adv.* **2015**, *5*, 81638.

[87] W. Hu, C. Peng, M. Lv, X. Li, Y. Zhang, N. Chen, C. Fan, Q. Huang, *ACS Nano* **2011**, *5*, 3693.

[88] G. Duan, S.-g. Kang, X. Tian, J. A. Garate, L. Zhao, C. Ge, R. Zhou, *Nanoscale* **2015**, *7*, 15214.

[89] a) R. Patil, P. Bahadur, S. Tiwari, *Adv. Colloid Interface Sci.* **2020**, *275*, 102051; b) A. M. Pinto, I. C. Gonçalves, F. D. Magalhães, *Colloids Surf., B* **2013**, *111*, 188.

[90] M. Peruzynska, K. Cendrowski, M. Barylak, M. Tkacz, K. Piotrowska, M. Kurzawski, E. Mijowska, M. Drozdzik, *Toxicol. In Vitro* **2017**, *41*, 205.

[91] I. Barbolina, C. R. Woods, N. Lozano, K. Kostarelos, K. S. Novoselov, I. S. Roberts, *2D Mater.* **2016**, *3*, 025025.

[92] H. Ali-Boucetta, D. Bitounis, R. Raveendran-Nair, A. Servant, J. Van den Bossche, K. Kostarelos, *Adv. Healthcare Mater.* **2013**, *2*, 433.

[93] A. F. Faria, F. Perreault, M. Elimelech, *ACS Appl. Nano Mater.* **2018**, *1*, 1164.

[94] L. Qi, T. Pan, L. Ou, Z. Ye, C. Yu, B. Bao, Z. Wu, D. Cao, L. Dai, *Commun. Biol.* **2021**, *4*, 214.

[95] D. W. Hwang, H. Y. Kim, F. Li, J. Y. Park, D. Kim, J. H. Park, H. S. Han, J. W. Byun, Y.-S. Lee, J. M. Jeong, K. Char, D. S. Lee, *Biomaterials* **2017**, *121*, 144.

[96] N. Panwar, A. M. Soehartono, K. K. Chan, S. Zeng, G. Xu, J. Qu, P. Coquet, K.-T. Yong, X. Chen, *Chem. Rev.* **2019**, *119*, 9559.

[97] R. Capelli, A. Gardin, C. Empereur-mot, G. Doni, G. M. Pavan, *J. Phys. Chem. B* **2021**, *125*, 7785.

[98] S. Ye, K. Shao, Z. Li, N. Guo, Y. Zuo, Q. Li, Z. Lu, L. Chen, Q. He, H. Han, *ACS Appl. Mater. Interfaces* **2015**, *7*, 21571.

[99] S. Zhu, F. Luo, B. Zhu, G.-X. Wang, *Toxicol. Res.* **2017**, *6*, 535.

[100] T. Malina, E. Maršálková, K. Holá, J. Tuček, M. Scheibe, R. Zbořil, B. Maršálek, *Carbon* **2019**, *155*, 386.

[101] S. Samadi, B. Asgari Lajayer, E. Moghiseh, S. Rodríguez-Couto, *Environ. Technol. Innovation* **2021**, *21*, 101323.

Yanyan Chen received her bachelor's degree from Shaanxi Normal University in 2014. In 2019, she obtained her Ph.D. from Institute of Chemistry, Chinese Academy of Sciences (ICCAS) under the supervision of Prof. Shu Wang. She is currently at Chalmers University of Technology as a postdoctoral fellow working with Prof. Ivan Mijakovic. Her research interests include design and synthesis of biocompatible nanomaterials for cell imaging, cancer therapy, antibacterial research, and intracellular catalysis. She is also interested in developing biological applications based on graphene and other 2D materials.

Santosh Pandit is a researcher at Chalmers University of Technology, Sweden. He obtained his Ph.D. from Chonbuk National University, Republic of Korea. His area of expertise includes bacterial biofilms, microbial resistant biomedical surfaces, and antimicrobial agents. His current research focuses on the antimicrobial coatings of graphene and other 2D materials on biomedical devices to prevent device-associated infections. His research also focuses on finding novel antimicrobial/anti-biofilm agents to prevent biofilm-associated infections as well as reducing the possibility of antimicrobial resistance development.

Ivan Mijakovic is a Chaired Professor of Bacterial Systems Biology at the Chalmers University of Technology, Sweden. He is also Professor and group leader at the Technical University of Denmark. He obtained his Ph.D. from the University Paris XI. He is an expert on bacterial protein phosphorylation and signaling, and his group investigates the physiology of bacterial model organisms and pathogens. Mijakovic' group also develops metabolic engineering strategies and new approaches to fight bacterial infections: novel antibacterial agents, coatings, and graphene-based sensors for infection.